Southwest Region University Transportation Center

Designing Fine Aggregate Mixtures to Evaluate Fatigue Crack-Growth in Asphalt Mixtures

SWUTC/11/161022-1

Center for Transportation Research
University of Texas at Austin
1616 Guadalupe St., 4th Floor
Austin, Texas 78701

Technical Report Documentation Page

1. Report No. SWUTC/11/161022-1	2. Government Accession No.	3. Recipient's Catalog No.
4. Title and Subtitle Designing Fine Aggregate Mixtures to Evaluate Fatigue Crack-Growth in Asphalt Mixtures		5. Report Date April 2011 6. Performing Organization Code
7. Author(s) Anoosha Izadi, Arash Motamed and Amit Bhasin		8. Performing Organization Report No. Report 161022-1
9. Performing Organization Name and Address Center for Transportation Research The University of Texas at Austin 1616 Guadalupe Street Austin, TX 78701		10. Work Unit No. (TRAIS) 11. Contract or Grant No. 10727
12. Sponsoring Agency Name and Address Southwest Region University Transportation Center Texas Transportation Institute Texas A&M University System College Station, TX 77843-3135		13. Type of Report and Period Covered 14. Sponsoring Agency Code
15. Supplementary Notes Supported by general revenues from the State of Texas		

16. Abstract

Fatigue cracking is a significant form of pavement distress in flexible pavements. The properties of the sand-asphalt mortars or fine aggregate matrix (FAM) can be used to characterize the evolution of fatigue crack growth and self-healing in asphalt mixtures. This study compares the internal microstructure of the mortar within a full asphalt mixture to the internal microstructure of the FAM specimen. This study also conducts a limited evaluation of the influence of mixture properties and methods of compaction on the engineering properties of the FAM specimens. The results from this study, although limited in number, indicate that in most cases the SGC compacted FAM specimen had a microstructure that most closely resembled the microstructure of the mortar within a full asphalt mixture. Another finding from this study was that, at a given level of damage, the healing characteristic of the three different types of FAM mixes was not significantly different. This indicates that the healing rate is mostly dictated by the type of binder and not significantly influenced by the gradation or binder content, as long as the volumetric distribution of the mastic was the same. In other words, the inherent healing characteristics of the asphalt binder plays a more significant role relative to other properties (e.g. volumetrics) in the overall fatigue cracking resistance of the asphalt mixture.

17. Key Words Asphalt, Sand-asphalt Mixture, Fine Aggregate Matrix, Fatigue, Self-healing	18. Distribution Statement No restrictions. This document is available to the public through the National Technical Information Service, Springfield, Virginia 22161.		
19. Security Classif. (of report) Unclassified	20. Security Classif. (of this page) Unclassified	21. No. of pages 54	22. Price

Form DOT F 1700.7 (8-72) Reproduction of completed page authorized

DESIGNING FINE AGGREGATE MIXTURES TO EVALUATE FATIGUE CRACK GROWTH IN ASPHALT MIXTURES

by

Anoosha Izadi
Arash Motamed
Amit Bhasin

Research Report SWUTC/11/161022-1

Southwest Region University Transportation Center
Center for Transportation Research
University of Texas at Austin
Austin, Texas - 78712

April 2011

DISCLAIMER

The contents of this report reflect the views of the authors, who are responsible for the facts and the accuracy of the information presented herein. This document is disseminated under the sponsorship of the Department of Transportation, University Transportation Centers Program, in the interest of information exchange. Mention of trade names or commercial products does not constitute endorsement or recommendations for use.

ACKNOWLEDGMENTS

The authors recognize that support was provided by a grant from the U.S. Department of Transportation, University Transportation Centers Program to the Southwest Region University Transportation Center which is funded, in part, with general revenue funds from the State of Texas. The authors would like to acknowledge the help of Mr. Swapneel Bedgaker for his assistance with designing some of the mixtures used in this study and Dr. Yong-Rak Kim from University of Nebraska - Lincoln, for serving as a Project Monitor for this study (three).

ABSTRACT

Fatigue cracking is a significant form of pavement distress in flexible pavements. The properties of the sand-asphalt mortars or fine aggregate matrix (FAM) can be used to characterize the evolution of fatigue crack growth and self-healing in asphalt mixtures. This study compares the internal microstructure of the mortar within a full asphalt mixture to the internal microstructure of the FAM specimen. This study also conducts a limited evaluation of the influence of mixture properties and methods of compaction on the engineering properties of the FAM specimens. The results from this study, although limited in number, indicate that in most cases the SGC compacted FAM specimen had a microstructure that most closely resembled the microstructure of the mortar within a full asphalt mixture. Another finding from this study was that, at a given level of damage, the healing characteristic of the three different types of FAM mixes was not significantly different. This indicates that the healing rate is mostly dictated by the type of binder and not significantly influenced by the gradation or binder content, as long as the volumetric distribution of the mastic was the same. In other words, the inherent healing characteristics of the asphalt binder plays a more significant role relative to other properties (e.g. volumetrics) in the overall fatigue cracking resistance of the asphalt mixture.

EXECUTIVE SUMMARY

Fatigue cracking is a significant form of pavement distress in flexible pavements. Fatigue crack growth and self-healing is predominantly concentrated in the sand-asphalt mortar or fine aggregate matrix (FAM) phase of the mixture. The Dynamic Mechanical Analysis (DMA) is typically used to characterize the performance and engineering properties of the FAM. Therefore the DMA of FAM specimens provides a magnified view of the fatigue cracking characteristics of the mixtures being investigated.

This study compares the internal microstructure of the mortar within a full asphalt mixture to the internal microstructure of the FAM specimen. The internal microstructures for three different types of FAM mixes, which were compacted using three different methods, were compared to microstructures of corresponding full asphalt mixtures. The metrics that quanitified the microstructure included the average star length distribution and the degree of anisotropy. These metrics were obtained by analyzing images acquired using the X-ray computed tomography. The results from this study, although limited in number, indicate that in most cases the SGC compacted FAM specimen had a microstructure that most closely resembled the microstructure of the mortar within a full asphalt mixture.

The second objective of this study was to examine the influence of mixture design characteristics (e.g. binder content and gradation) on the engineering properties of the FAM mixes. The DMA was used to determine the linear viscoelastic properties of the FAM specimens. Time sweep tests at high stress amplitudes were conducted to determine the fatigue cracking characteristics of the FAM specimens. The fatigue cracking characteristics of the FAM specimens were strongly influenced by the binder content; the percentage of fines did not have a significant influence. The DMA was also used to determine the self-healing characteristics of the FAM specimens. Results indicate that the rate of healing quantified as the change in linear viscoelastic complex shear modulus for a given level of damage was very similar irrespective of the loading history. Results also indicate the healing characteristics of the three different types of FAM mixes were not significantly different. This indicates that the healing rate was mostly dictated by the type of binder and not significantly influenced by the gradation or binder content, provided that the volumetric distribution of the mastic is the same.

TABLE OF CONTENTS

LIST OF FIGURES

LIST OF TABLES

CHAPTER 1. INTRODUCTION

1.1 PROJECT BACKGROUND

Fatigue cracking is a significant form of pavement distress in flexible pavements. The most common method to quantify the resistance of asphalt mixtures to fatigue cracking and other distress mechanisms is by performing mechanical tests under controlled laboratory conditions on mixture specimens. The advantage of this approach is that candidate mixtures can be ranked based on their performance using a simple laboratory test. Another advantage of this approach is that it takes into account the combined affect of material and mixture properties on mixture performance. However, there are three major limitations to this approach. First, it does not provide any information that can be used to explain why certain mixtures perform better than others. This in turn limits the ability of the engineer to take cost effective remedial actions to improve the performance of poor performing mixtures. Second, the evolution of damage from some of the traditional laboratory performance tests is dependent on the test conditions (e.g. specimen geometry or mode of loading) and cannot be extrapolated to field conditions. Finally, the results obtained by conducting tests on full asphalt mixtures often have a very high variability.

To alleviate some of these shortcomings, several research studies have been undertaken to investigate the properties and performance of asphalt mixtures at multiple length scales. For example, constituent materials (e.g. binder, aggregate, and fines) are evaluated in order to identify their contribution to mixture properties and damage evolution. Properties of mastics (fines mixed with asphalt binder) are evaluated to understand filler-binder interactions. Evaluation of sand-asphalt mortars or FAM provides information on the evolution of damage in this phase, role of fines to arrest crack growth, and moisture damage. Evaluation of full asphalt mixtures helps identify the role of coarse aggregate properties and mixture microstructure in resistance of the mixture to damage.

The Dynamic Mechanical Analysis (DMA) is typically used to characterize the performance and engineering properties of the fine aggregate matrix or the sand-asphalt mortar, hereafter referred to as fine aggregate matrix (FAM) for brevity. Distresses such as fatigue crack growth are concentrated in the sand-asphalt mortar or FAM phase of the mixture (Kim and Little, 2005). Therefore the DMA of FAM specimens provides a magnified view of the fatigue cracking characteristics of the mixtures being investigated. This approach can be used to (i) evaluate the response and rank the performance of different material

combinations, (ii) evaluate the efficacy of using additives such as warm mix agents, liquid anti-strip agents or hydrated lime, and (iii) provide required mechanical properties as an input for computational modeling of full asphalt mixtures (Kim et al., 2003, 2004; Kim and Little, 2005; Masad et al., 2006; Branco et al., 2008; Caro et al., 2008). For each of the aforementioned applications, it is important that the FAM represent the design and internal structure of the sand-asphalt mortar phase from the full asphalt mixture as closely as possible. A short review of the some of the methods to design and fabricate the FAM specimens is presented below.

Kim et al. (2003) reported the use of sand-asphalt mixture to evaluate the influence of fillers such as hydrated lime and limestone fines on the rheological properties of the asphalt binder and the mix. They used different filler to asphalt binder ratios and Ottawa sand to produce the sand-asphalt mixtures. They also measured the linear viscoelastic properties of these mixtures and subjected the test specimens to a time sweep or fatigue test using a Dynamic Shear Rheometer (DSR). The results from these tests were used with continuum mechanics to quantify the influence of different fillers on the performance of different asphalt binders. Kim et al. used fine aggregates as a carrier to fabricate mortar specimens with different filler to binder ratios. In studies that followed Kim et al., researchers replicated the mortar (in terms of the material and gradation) from a specific full asphalt mixture in lieu of using a standard fine aggregate (such as Ottawa sand) to fabricate FAM specimens. The two main advantages of this approach are:

1. The mechanical properties and physio-chemical interactions between the aggregate and binder are replicated in the FAM specimen. Consequently, the damage evolution of the mortar specimens can be measured and used as a material screening tool for the design of optimal performing mixtures.

2. The mechanical properties and the damage evolution in the FAM specimens can be measured and used as an input for computational models to determine the response of full asphalt mixtures.

For example, Zollinger (2005) selected the fine aggregates and gradation from eight different asphalt mixtures with known field performance. The gradation of the fine aggregates (in this case defined as aggregates passing 1.18 mm sieve) in the FAM followed the same proportions as that of the selected full asphalt mixture and the binder content was selected such that the volume of filler (fines passing number 200 sieve) was 10 percent the volume of the binder. Zollinger (2005) used a Superpave Gyratory Compactor (SGC) to compact a

six inch diameter and approximately three inch tall mortar specimen with a target air void content of eleven percent. Approximately twenty test specimen, two inch in height and 1/2" in diameter, were obtained by sawing and coring each SGC compacted specimen. The fatigue cracking life of the FAM specimens for the eight different asphalt mixtures were tested with and without moisture conditioning. Results were shown to correlate well with the observed field performance of these mixtures. Caro et al. (2008) also used a similar approach to design FAM specimens to evaluate the moisture sensitivity of five different asphalt mixtures and the contribution of hydrated lime to improve the moisture damage resistance of certain mixtures. Masad et al. (2006) and Branco et al. (2008) used a similar approach with a slight modification to characterize the fatigue cracking life under different modes of loading for FAM specimens. Instead of using a constant binder to filler volume ratio, Branco et al. (2008) adjusted the binder content to reflect the binder content within the mortar phase of the full asphalt mixture. In other words, the mass percent of the binder in the FAM was the same as the percentage of binder by mass of fine aggregates in the full asphalt mixture.

In summary, several different approaches have been suggested to design the FAM based on the mixture design of a full asphalt mixture. However, there is no evidence to support the premise that the microstructure of the sand-asphalt mixtures fabricated in the laboratory is similar to the microstructure of the sand asphalt portion of a full asphalt mixture. Different researchers have used different approaches to design the FAM mixtures based on different assumptions. This is a significant knowledge gap that must be addressed to allow proper design of FAM mixtures, in order to have a meaningful and accurate relationship to full mixture properties and performance modeling.

1.2 OBJECTIVES

The two objectives of this study were to: (i) compare the internal microstructure of the mortar from a full asphalt mixture to the internal microstructure of the FAM specimen for different mix designs, (ii) to evaluate whether the method of compaction used to fabricate FAM specimens had any influence on its mechanical properties, and (iii) to evaluate the influence of mixture design characteristics such as gradation and binder content on the performance of the FAM specimens. These objectives were achieved by accomplishing the following key steps.

- Asphalt mixture specimens with different aggregate gradations and binder contents

were fabricated in the laboratory using the Superpave Gyratory Compactor. FAM specimens replicating the designs from the full asphalt mixtures were fabricated using three different compaction methods.

- Representative volumes of the full asphalt mixtures as well the FAM specimens were scanned using very high resolution three-dimensional X-ray computed tomography (X-Ray CT). The objective of this task was to compare the three dimensional microstructure of the mortar from a full asphalt mixture to the microstructure of a FAM specimen representing a comparable mix design. Consequently, smaller representative portions of the full asphalt mixture specimen were scanned using very high resolution X-ray CT instead of lower resolution scans of full asphalt mixture specimens. Specimens and scanned images for the full asphalt mixtures were available from a previous study. The star length distribution (SLD) was selected as a metric to compare the internal microstructure of the FAM specimens to the internal microstructure of the mortar from the full asphalt mixture.

- Mechanical properties of the FAM specimens, including stiffness, fatigue cracking resistance, and propensity to heal were measured using the DMA. These properties were compared for FAM specimens with similar mix designs compacted using different methods as well as FAM specimens with different mix designs.

1.3 REPORT STRUCTURE

This report consists of five chapters. The first chapter in on the project background and objectives of this study. The second chapter presents the necessary background on metrics to quantify the microstructure based on analysis of images obtained using X-Ray CT. This chapter also presents the relevant background on the use of DMA to determine stiffness, fatigue cracking resistance and healing characteristics of the mortar specimens. The third chapter presents the experimental design, methodology used to fabricate specimens, collection and processing of data and the results obtained. Chapter four presents a discussion of findings and conclusions from this study.

CHAPTER 2. BACKGROUND AND LITERATURE REVIEW

2.1 METRICS TO CHARACTERIZE THE INTERNAL MICROSTRUCTURE

The term internal structure of an asphalt concrete mixture refers to the content and spatial distribution of asphalt, aggregates and air-voids (Masad et al., 1999). The internal structure of the mixture is dictated by the proportions and properties of its constituent materials and method of compaction. It is well recognized that the internal structure of an asphalt mixture plays a significant role in influencing the mechanical properties and the resistance of the mixture to major distresses including rutting, fatigue cracking, thermal cracking and low temperature cracking. Most mixture design methods recognize the importance of internal microstructure by imposing requirements for aggregate size, gradation, shape, density during compaction and volumetrics (Masad and Button, 2004).

In a previous study, Bhasin et al. (2009) used X-ray CT images to determine the three dimensional fabric tensor of the mastic in the mortar portion of a full asphalt mixture. They used the fabric tensor and star length distribution to compute the degree of anisotropy, average star length in the preferred direction, orientation of the preferred direction, and average coefficient of variation of star lengths along different directions. In this study, these metrics will be used to compare the internal microstructure of the mortar portion of a full asphalt mixture to the internal microstructure of an equivalent FAM specimen. A summary of the procedures to compute and interpret these metrics is presented in this section while details on the application of these metrics to characterize the microstructure of asphalt mixtures can be found in Bhasin et al.

The metrics described above are determined using digital images acquired using a high resolution X-ray CT scanning. Grayscale digital images obtained using the X-ray CT scanning typically contain some amount of noise and must be preprocessed prior to being used for analysis. The typical steps involved in pre-processing are cropping the images to appropriate size, noise reduction, and thresholding to differentiate between the different components in the image (binder or mastic, air voids, and aggregates). The post processed images are then used for image analysis.

A continuous quantity that varies with orientation can be used to quantify the orientation and distribution of material objects within a composite. In this study, the star length distribution (SLD) was used to characterize the internal microstructure of the asphalt mixture. The star length distribution is calculated by randomly selecting several points in the

material of interest within the composite and measuring the length of lines emanating from these points in various directions until the lines encounter a boundary (Odgaard, 1997). By doing so, the distribution of the material of interest is obtained. The orientations along which the lines emanate from the points are typically predefined by selecting a homogeneous distribution of points on a unit sphere. Increasing the number of points reduces the uncertainty and is more efficient than increasing the number of orientations. The average star length along an given orientation is computed as:

$$S_w = \frac{1}{n}\sum_{i=1}^{n} L_i \tag{2.1}$$

where, L is the length of measured intercept through point i at orientation w and n is the number of points. The SLD can be obtained for any single material that is of interest within a multi-component composite. Figure 2.1 illustrates in two dimensions the measurement of star length in a two component composite along eight orientations at four randomly selected points. The average star length is then computed along each one of the eight directions using equation 2.1. A two dimensional rose diagram for the mean star length along different directions provides a visual representation of the internal microstructure.

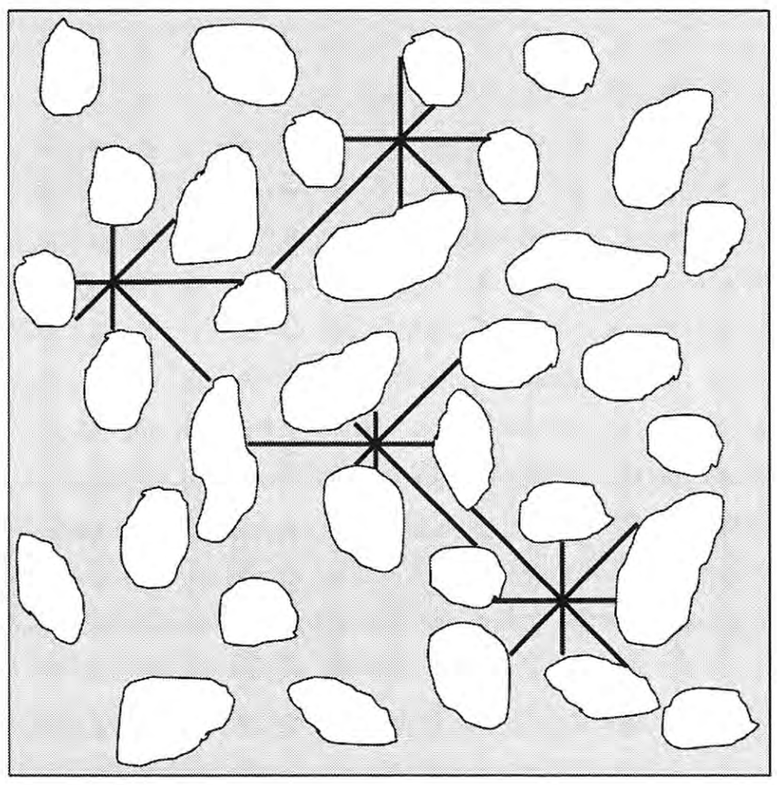

Figure 2.1. Schematic Illustrating Measurement of Star Length for a Two Component Composite in Two Dimensions.

In this study, the three dimensional star length distribution was used to characterize the geometry of the mastic within the mortar of the full asphalt mixture. Although a three dimensional rose diagram of the mean star length provides a visual representation of the

geometry, it is also important to reduce this information into quantitative parameters that relate to the mechanical properties of the composite. One such parameter, that will be used later to characterize the microstructure of sand-asphalt mixtures, is the fabric tensor based on the moment of inertia. Consider that the star lengths are measured at n points along w orientations to produce a data set of N vectors represented by $\mathbf{a}_i$, where $i = 1$ to N.

$$\mathbf{a}_i = \begin{bmatrix} a_{xi} \\ a_{yi} \\ a_{zi} \end{bmatrix} \tag{2.2}$$

Watson (1966) proposed that the orientation matrix or fabric tensor for this data set is mathematically obtained as follows.

$$\mathbf{T} = \sum_{i=1}^{N} \mathbf{a}_i \mathbf{a}_i^T = \begin{bmatrix} \sum_{i=1}^{N} a_{xi}^2 & \sum_{i=1}^{N} a_{xi}a_{yi} & \sum_{i=1}^{N} a_{xi}a_{zi} \\ \sum_{i=1}^{N} a_{xi}a_{yi} & \sum_{i=1}^{N} a_{yi}^2 & \sum_{i=1}^{N} a_{yi}a_{zi} \\ \sum_{i=1}^{N} a_{xi}a_{zi} & \sum_{i=1}^{N} a_{yi}a_{zi} & \sum_{i=1}^{N} a_{zi}^2 \end{bmatrix} \tag{2.3}$$

The orientation matrix or fabric tensor $\mathbf{T}$ has three eigenvalues $\hat{\tau}_1 > \hat{\tau}_2 > \hat{\tau}_3$ and corresponding eigenvectors $\hat{\mathbf{u}}_1$, $\hat{\mathbf{u}}_2$, $\hat{\mathbf{u}}_3$ (Watson, 1966; Ketcham, 2005b). For any axis represented by vector $\mathbf{u}$, the moment of inertia $I(\mathbf{u})$ is given by equation 2.4.

$$I(\mathbf{u}) = \sum_{i=i}^{N} |a_i|^2 - \mathbf{u}^T \mathbf{T} \mathbf{u} \tag{2.4}$$

Finally, the eigenvectors $\hat{\mathbf{u}}_1$ and $\hat{\mathbf{u}}_3$ also represent the direction vectors along which the moment of inertia is minimized and maximized, respectively. The eigenvectors can be used to derive important parameters that reflect the properties of the composite. For example, the degree of anisotropy, DA, can be computed as (Ketcham, 2005b):

$$DA = \hat{\tau}_1 / \hat{\tau}_3 \tag{2.5}$$

and elongation index, EI, as:

$$EI = 1 - (\hat{\tau}_2 / \hat{\tau}_1) \tag{2.6}$$

2.2 METRICS TO CHARACTERIZE MECHANICAL PROPERTIES OF MORTAR SPECIMENS

Mortar specimens comprise asphalt binder and fine aggregates passing #16 sieve. Typically, the test is conducted using a dynamic shear rheometer (DSR) in torsion shear mode. DMA is used in many fields such as engineering, chemistry and polymer physics. This technique is also referred to as forced oscillatory measurements, dynamic mechanical thermal analysis (DMTA), dynamic thermo mechanical analysis or dynamic rheology. DMA can be defined as a technique of applying an oscillatory or pulsing force to a sample. Its importance can be explained by the fact that it provides information on the ability of viscoelastic materials to store and dissipate mechanical energy upon deformation.

In the context of this research, the dynamic mechanical analysis (DMA) of mortar specimens refers to the characterization of damaged and undamaged properties of the mortar. The undamaged properties refer to creep compliance or relaxation modulus of the material as a function of time and temperature or dynamic modulus of the material as a function of frequency and temperature. Damaged properties include rate of plastic deformation, fatigue crack growth, moisture induced damage and also propensity of the material to self-heal. The methods to determine the undamaged properties are well established in the literature. For example, methods to measure and mathematically model the creep compliance or dynamic modulus are well described in the literature (Ferry, 1980; Wineman and Rajagopal, 2000; Lakes, 2009; Brinson and Brinson, 2008). In this study, the dynamic shear modulus and accompanying phase angle were used as indicators of undamaged properties.

There are a number of metrics that have been used to characterize the damage characteristics of mortars or other viscoelastic composites in the literature. A very brief review of some of these methods is presented below. The discussion is limited to the most common types of distress experienced by bituminous materials.

2.2.1 Plastic deformation in a specimen

Plastic deformation in a viscoelastic material is a function of the load, loading time, and temperature. Typically a series of creep load tests are conducted to measure the recoverable (delayed elastic also referred to as viscoelastic in the context of bituminous materials) and irrecoverable plastic deformation in the material. The resulting response can be mathematically modeled in a form that quantifies the amount of plastic deformation as a function of the load and loading time. There are several mathematical models that are available to

achieve this. For example, a mechanical model with a friction element that is characteristic of the yield stress can be used. If the applied stress exceeds the characteristic yield stress of the friction element, the material deforms. Unlike the elastic spring or the viscous dashpot, that are also used in the mechanical models, the friction element does not have a well-defined constitutive equation. Therefore, it is typically used in combination with another element. Another approach that is more commonly used is the extension of the classical yield theories or criteria to incorporate time dependency. For an elasto-plastic material a general form of the yield criteria or surface can be written as:

$$f\left(\sigma_{ij}, \varepsilon_{ij}^{p}\right) \geq 0 \tag{2.7}$$

where, σ_{ij} is the stress tensor and ε_{ij}^{p} is the plastic strain tensor used in lieu of the failure stress. For elasto-viscoplastic materials, the time dependency is accommodated by using an additional parameter. For example equation 2.7 can be modified as follows:

$$f\left(\sigma_{ij}, \varepsilon_{ij}^{p}, \tau_{ij}\right) \tag{2.8}$$

where, the term τ_{ij} adjusts the yield criterion accordingly to accommodate for the viscoelastic nature of response. One example is the Nagdi-Murch model that defines this term as follows:

$$\tau_{ij} = \tau_{ij}\left(\varepsilon_{ij}^{v} - \varepsilon_{ij}^{e}\right) \tag{2.9}$$

where, ε_{ij}^{v} and ε_{ij}^{e} denote the time dependent and elastic strains, respectively. Crochet (1966) defined the time dependent function to be a scalar of the form:

$$\tau = \sqrt{\left(\varepsilon_{ij}^{v} - \varepsilon_{ij}^{e}\right)\left(\varepsilon_{ij}^{v} - \varepsilon_{ij}^{e}\right)} \tag{2.10}$$

More recently, Masad and co-workers have used the Schapery's nonlinear viscoelastic model to characterize the nonlinear viscoelastic and viscoplastic strain in asphalt materials (Masad et al., 2008; Huang et al., 2007). They were able to quantify the evolution of plastic strain in the asphalt specimen by accounting for stress history and the delayed elastic or viscoelastic strain from a multiple creep load test.

2.2.2 Fatigue crack growth

Cyclic or monotonic load tests are typically conducted to determine fatigue cracking or fracture resistance of the material. Most of the work related to crack growth in bituminous materials is centered around two approaches; the energy-based path-independent integrals and the cohesive zone model. Cherepanov (1968) and Rice (1968) developed the energy based integral approach, now commonly referred to as the J-integral approach, to define the work done per unit area of crack growth. Schapery (1975a; 1975b; 1975c; 1984) used the energy-based path independent J-integral for non-linear elastic and plastic materials in conjunction with correspondence principles to derive an expression for crack initiation and crack growth in a viscoelastic media.

Masad et al. (2006) used the correspondence principle proposed by Schapery (1984) and the DMA to characterize fatigue damage in mortars. DMA samples were compacted and cored according to the procedure described by Zollinger (2005). DMA tests were performed under controlled-strain and controlled-stress modes of loading, 25°C, and 10Hz frequency. The tests were done in two stages: a low amplitude test was conducted to determine the undamaged or linear viscoelastic properties followed by a high amplitude test to induce fatigue cracking. The authors observed that controlled-strain and controlled-stress tests develop fatigue cracking in a different way. Under controlled-strain, the strain is kept constant and the stress decreases during the test. The dynamic modulus decreases, while the phase angle increases. These two modes of testing have an opposite influence on the area of the hysteresis loop (the fact that the dynamic modulus decreases makes the area of the hysteresis loop to decrease and the fact that the phase angle increase makes the area of the hysteresis loop to increase). The net effect is that in controlled-strain the hysteresis loop area decreases during the test and under controlled-stress test conditions, both manifestations of damage (decrease in stiffness and increase in phase angle) have the same effect; increase the hysteresis loop area. The approach proposed by these authors was to separate the dissipated energy due to the fatigue damage into three main sources: (i) the change in the phase angle (WR1), (ii) permanent deformation involved in the process (WR2) and (iii) the change in the mix stiffness (WR3). The authors found that using intermediate values of dynamic modulus and phase angle (within the nonlinear region) as the viscoelastic properties (VE) they were able to separate the effects of the nonlinear material behavior and the damage. Bhasin et al. (2009) compared the use various energy based methods to quantify the rate of fatigue crack growth in asphalt mixtures.

2.2.3 Moisture damage

The presence of moisture in mortar or asphalt mixture specimens amplifies other forms of distress such as fatigue crack growth. The moisture damage potential of mortar specimens is typically determined in conjunction with the fatigue crack growth. Zollinger (2005) compared the fatigue cracking resistance of moisture conditioned specimens to unconditioned specimens using the DMA in order to evaluate their moisture damage resistance. Moisture conditioning was achieved by allowing moisture to penetrate the specimen by placing it in distilled water and applying vacuum to accelerate moisture penetration. The specimen was retained under water and vacuum for one hour. Zollinger (2005) reported that the saturation computed as the volume of water absorbed to the volume of air voids, was approximately 125 percent indicating that some of the moisture diffused into the binder or aggregate matrix. Caro et al. (2008) used a similar approach to characterize the moisture damage resistance of mortar specimens. They compared the performance of moisture conditioned specimens to unconditioned specimens and quantified the moisture damage resistance using a probabilistic approach.

2.2.4 Healing potential

Some of the recent work on the laboratory investigation of healing can be attributed to Little et al. (2001), Kim and Roque (2006), Carpenter and Shen (2006) and Maillard et al. (2004). These studies clearly demonstrate the evidence for existence of healing and its significant impact on the fatigue cracking life of asphalt mixtures. Little et al. (2001) applied a rest period of 24-hours in traditional flexural beam bending experiments resulting in the increase of fatigue life by more than 100 percent depending on the type of binder used. Kim and Little (2005) used torsion loading on asphalt mastics to demonstrate similar results. They observed that the impact of healing is by far the greatest when rest periods are applied before significant damage occurs. Carpenter and Shen (2006) used dissipated energy between load cycles to quantify healing. They verified this observation by demonstrating that the application of short rest periods between each load cycle not only extends fatigue life but is also responsible for the extension of so called "endurance limit" of some asphalt mixtures. Kim and Roque (2006) quantified healing in terms of the recovered dissipated creep strain energy per unit time by using similar approach as that of Carpenter and Shen (2006). Maillard et al. (2004) simulated the conditions in which an asphalt film is bound by aggregates by conducting tensile tests on films of asphalt binders lodged between glass spheres. Rate

of healing in the asphalt was measured by transmitting ultrasonic waves through the sample. A decrease in the amplitude of the ultrasonic signal corresponds to damage in the film whereas an increase in the amplitude corresponds to the healing process.

Similar to the work of Kim and Little (2005), Bhasin et al. (2008) quantified the healing potential of different FAM mixtures using the DMA. They applied cyclic loads to FAM specimens using a DMA and introduced nine rest periods of four minutes each during the cyclic test. The rest periods were introduced after cycles that correspond to 2.5, 5, 10, 15, 20, 25, 30, 40, and 50 percent of the fatigue life value for that particular material, as measured without any rest period. When rest periods were applied, the parameter, b, was computed as the slope of the dissipated energy versus ln number of load cycles. The parameter b determined without the rest period was then compared to the parameter b determined with rest periods. A relative decrease in this parameter, which would be associated with positive healing, was then used to quantify the healing potential for each material.

2.3 METRICS USED IN THIS STUDY

In this study, the DMA is used to evaluate whether the method of compaction used to fabricate FAM specimens has any influence on its mechanical properties and to evaluate the influence of mixture design characteristics such as gradation and binder content on the performance of the FAM specimens. Due to the limited scope, not all the metrics described in the aforementioned sections were included in this study. A summary of parameters that were used to compare the microstructure and engineering properties of the specimens is listed below. A more detailed description on how these metrics were obtained for the selected materials is presented in Chapter 3.

Parameters for the full asphalt mixture specimens as well as the FAM specimes based on the image analysis of microstructure include the following.

1. Degree of anisotropy (equation 2.5).
2. Average star length along the principal direction (equation 2.1).
3. Average coefficient of variation of the star lengths along all directions.
4. Orientation of the principal direction (equation 2.3).

Parameters for the FAM specimens based on the mechanical tests include:

1. Undamaged shear dynamic modulus or G* and phase angle.

2. Rate of crack growth from a fatigue test.

3. Healing characteristics during long rest periods.

CHAPTER 3. MATERIALS, TESTS AND RESULTS

The previous chapter presented a summary from the literature review on metrics to characterize the internal structure of the FAM portion in full asphalt mixtures as well as metrics to characterize fatigue crack growth and self-healing characteristics of FAM specimens using the DMA. The following sections of this chapter present more details on the materials and methods used to fabricate test specimens and imaging of the specimens using the micro X-ray CT scanner and testing of the specimen using the DMA.

3.1 SELECTION OF MATERIALS AND SPECIMEN FABRICATION

The primary objective of this study was to evaluate the influence of mixture properties and methods of compaction on the properties of the FAM. A secondary objective of this study was to compare the microstructure of the FAM specimen to the microstructure of the FAM portion of a corresponding full asphalt mixture. To achieve the objective of this study, a typical dense graded asphalt mixture was selected. Three additional variations of this mixture were produced in the laboratory by changing the binder content, coarse aggregate gradation, and fine aggregate gradation to produce a total of four different mixtures. The four mix designs were labelled as control, high binder, coarse adjusted, and fine adjusted. The aggregate used in all mixtures was a limestone obtained from RTI South Plant, Buda, Texas. Limestone is well suited for X-ray CT scanning because of its relatively homogeneous mineral makeup compared to other aggregates. Although igneous aggregates or gravels may also be used, these aggregates typically contain minerals with varying densities that may result in non-uniform X-ray attenuation and artifacts in the CT images. The asphalt binder had a performance grade of PG 64-22.

Figure 3.1 illustrates the gradation and binder content for these four mixtures. The gradation limits were based on the specification followed by the Texas Department of Transportation (TxDOT) for Type C mixtures and all variations of the control mix were designed to be within these limits. The *control mix* had 4.2% binder content by weight of aggregates, and the *high binder* mix had 4.7% binder content but the same aggregate gradation as the control mix. The coarse adjusted mix had the same binder content and fine aggregate (passing #16 sieve) gradation as the control mix but the gradation of the coarser aggregates (retained on #16 sieve) was modified. Similarly, the fine adjusted mix had the same binder content and coarse aggregate gradation as the control mix but the fine aggregate

gradation was modified. Three different types of FAM mix designs were also developed corresponding to the control (labelled as Mix 1), high binder (labelled as Mix 2), and fine adjusted (labelled as Mix 3) full mixtures. A FAM mix design for the coarse adjusted full mixture was not developed because of the following reason. The coarse adjusted mix had a gradation that was adjusted only in the coarse aggregate fraction (aggregate retaining on #16 sieve) as compared to the control mix. In other words, the gradation of the aggregates passing #16 sieve was the same for the coarse adjusted mix as well as the control mix. As a result, the gradation for the FAM mix corresponding to both these mixtures was the same. Appendix A presents an example illustrating the methodology that was used to determine a FAM mix design corresponding to the design of a full asphalt mixture. Figure 3.2 illustrates the gradations for the three FAM mixtures.

It is important to emphasize that all four mixes used the same binder and aggregate and only difference between the control and other mixes was either the binder content or the gradation. The rationale for selecting these four mixtures was to evaluate the influence of binder content and gradation on the properties of the FAM specimen as well as to compare the microstructure of the FAM specimen to the microstructure of the FAM within a corresponding full asphalt mixture.

The maximum specimen size that can be used with the three dimensional X-ray CT scanner is dictated by the resolution required for micro structure characterization. A resolution in the range of 15 micrometers per voxel was considered as appropriate for this study. A cylindrical specimen approximately 12.5 mm in diameter was considered as appropriate to achieve this resolution. This specimen diameter was also appropriate for the mechanical testing using the DMA. The following procedure was used to obtain specimens for the full asphalt mixture for X-ray CT scanning and specimens for FAM mixtures for X-ray CT scanning and DMA testing.

Full asphalt mixture specimens for each of the four mixture types were compacted using the Superpave gyratory compactor (SGC). The specimens were 152 mm in diameter and 100 mm in height. The ends of the SGC compacted specimen were cut using a diamond blade saw to achieve a finished specimen height of 50 mm. A diamond coring bit was used to core approximately ten specimens that were half inch in diameter and 50 mm in height. Two specimens cored from the SGC compacted specimen for each type of mixture were selected for X-ray CT scanning. The two cored specimen were selected so that they had similar air void content as compared to the average air void content of the SGC compacted specimen.

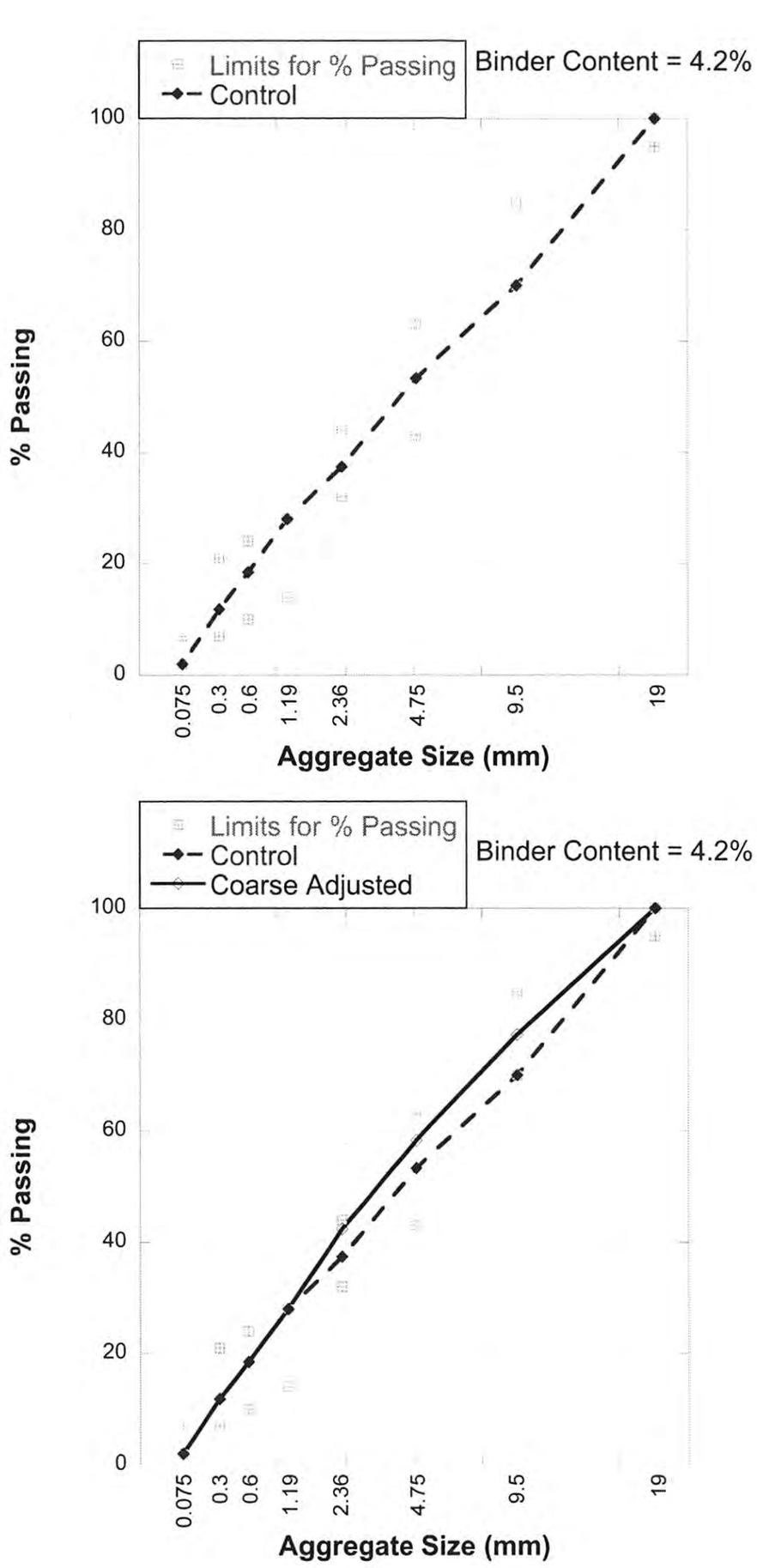

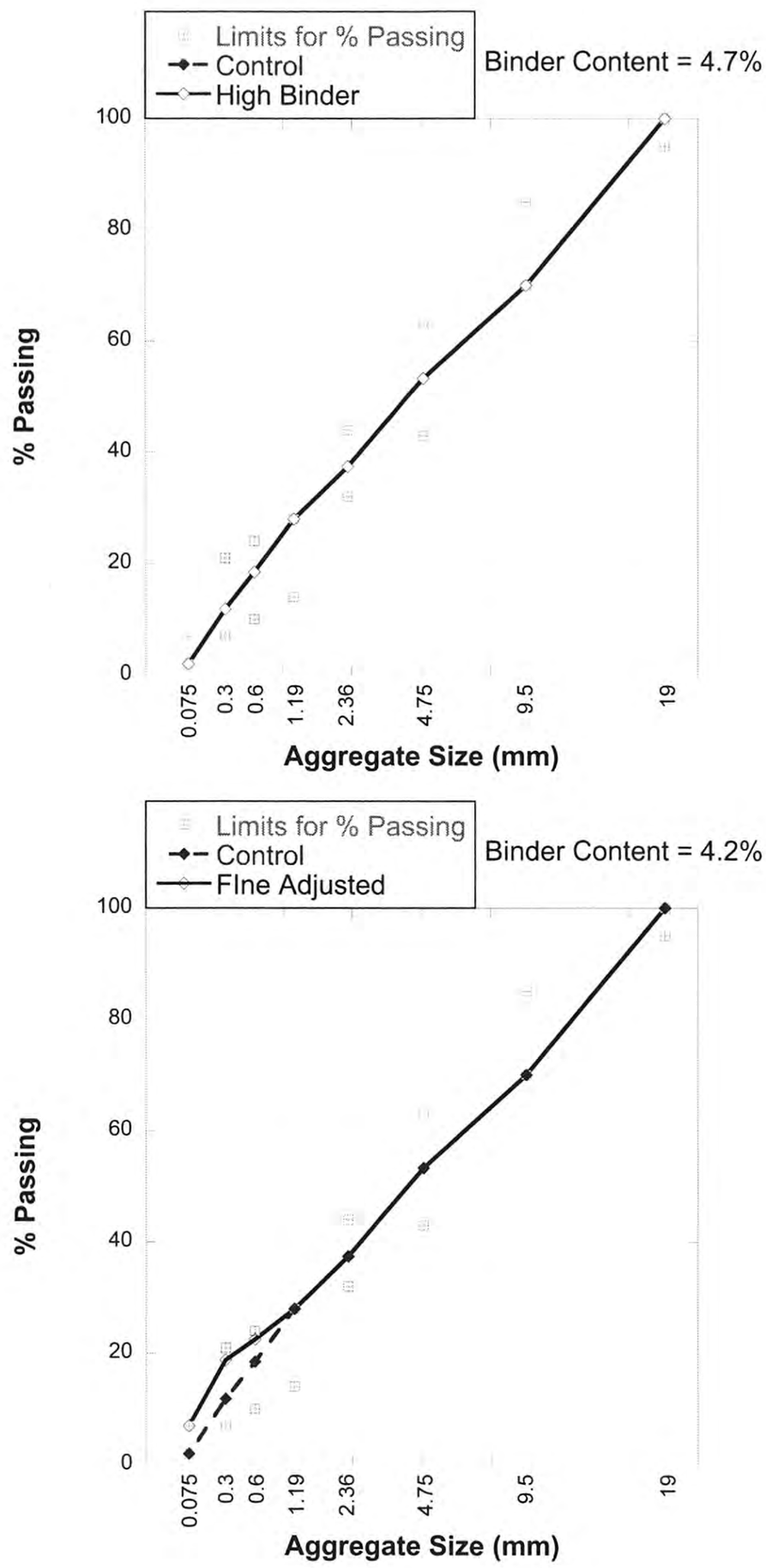

Figure 3.1. Gradations for the Four Different Full Asphalt Mixtures.

The cylindrical FAM test specimen comprised of the bitumen mixed with fine aggregate (material passing #16 sieve). The aggregates and the bitumen were mixed at the specified mixing and compaction temperature using a mechanical mixer. After short term aging for two hours, the mix was compacted using three different methods. The first method was to use a 152 mm diameter mold with the Superpave gyratory compactor to compact a specimen with a height of 75 mm and target air void content of 13%. The compacted samples were allowed to cool to room temperature. Each side of the compacted sample

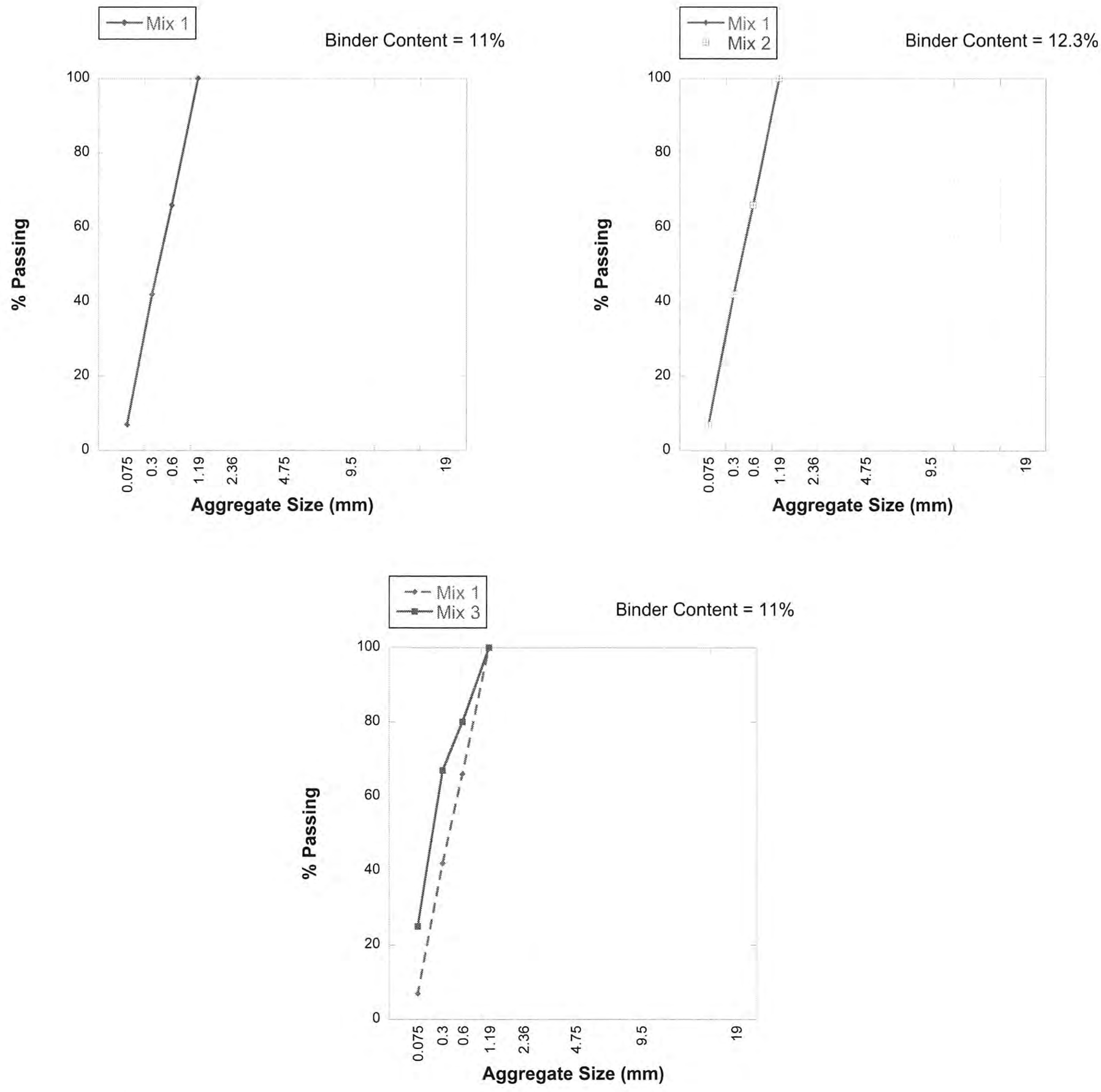

Figure 3.2. Gradations for the Three Different FAM Mixtures.

(top and bottom) was trimmed to obtain a sample height of 50 mm. Approximately 30 FAM test specimens of 12.5 mm diameter were obtained by coring the 152 mm diameter compacted sample. FAM specimens from the inner core of the SGC compacted specimen were separated from the specimens from the outer core of the SGC compacted specimen. Figure 3.3 illustrates the schematic of these specimens.

The second method was to use a beam compactor. The short term aged loose mix was compacted using a beam compactor and test specimen. The beam specimen was trimmed

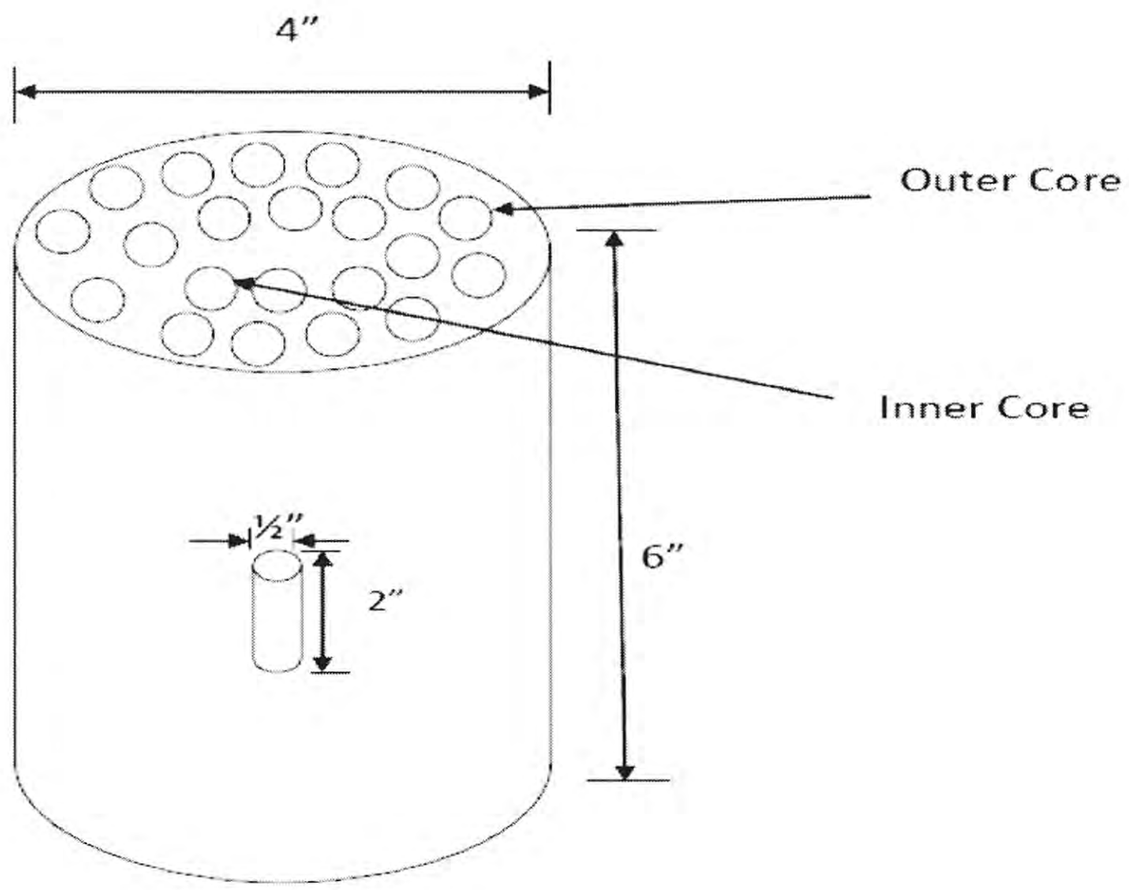

Figure 3.3. Schematic of FAM Specimens Cored out of SGC Specimen.

by about 15 mm from all sides to reduce end effects. FAM test specimens were then cored from the beam specimen by coring in the direction of compaction as well as perpendicular to the direction of compaction. Figure 3.4 illustrates a schematic for the FAM specimens obtained using the beam compacted specimen. The third and last method of compaction was to use a Marshal compactor. The procedure was the same as the SGC specimen but the FAM specimens were obtained only from the middle part of the specimen and hence there were no inner or outer core specimens. It must be noted that all specimens were compacted until refusal, i.e. the compaction effort was applied until no change in volume of the specimen was observed.

3.2 CHARACTERIZING THE MICROSTRUCTURE

The finished full mix and FAM specimens were used to obtain high resolution sectional images for a volume of interest. The scanning was performed at the high-resolution X-ray CT Facility at the University of Texas at Austin (UTCT). Ketcham and Carlson (2001) provide a more detailed description of the principles of X-ray tomography and methods used to acquire images and correct artifacts. In summary, high-resolution X-ray CT scanning (HRXCT) is based on the principle that an X-ray fan beam (or cone beam) is directed at an object from all orientations in a plane. The decrease in X-ray intensity caused by passage through the object is measured by a linear array of detectors (Figure 3.5). The resulting

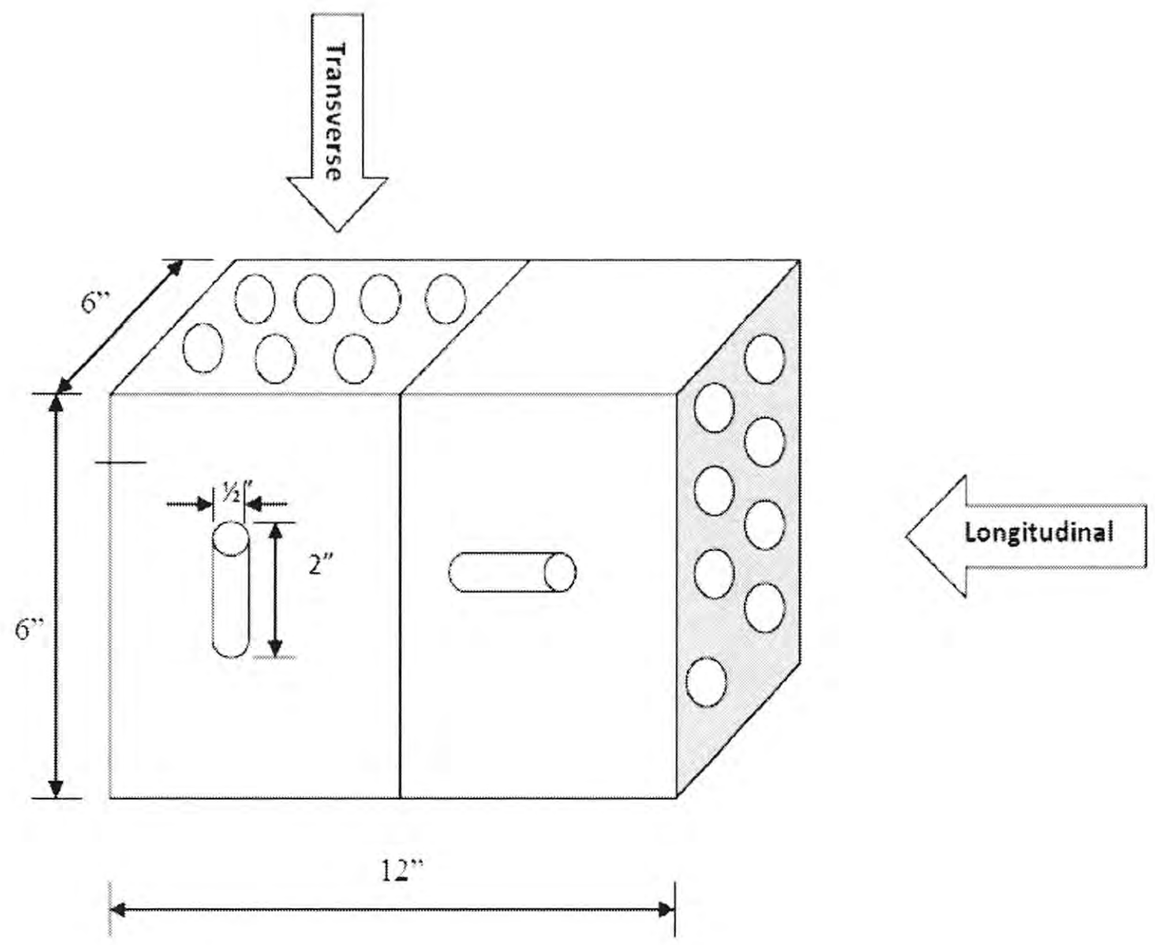

Figure 3.4. Schematic of FAM Specimens Cored out of Beam Specimen.

data are then reconstructed to create a cross-sectional image of the object along that plane. The gray scales in such images reflect the relative linear X-ray attenuation coefficient μ, which is a function of density, atomic number, and X-ray energy. For this study, the energy source used was adjusted to 80kV and 10W to obtain the best resolutions.

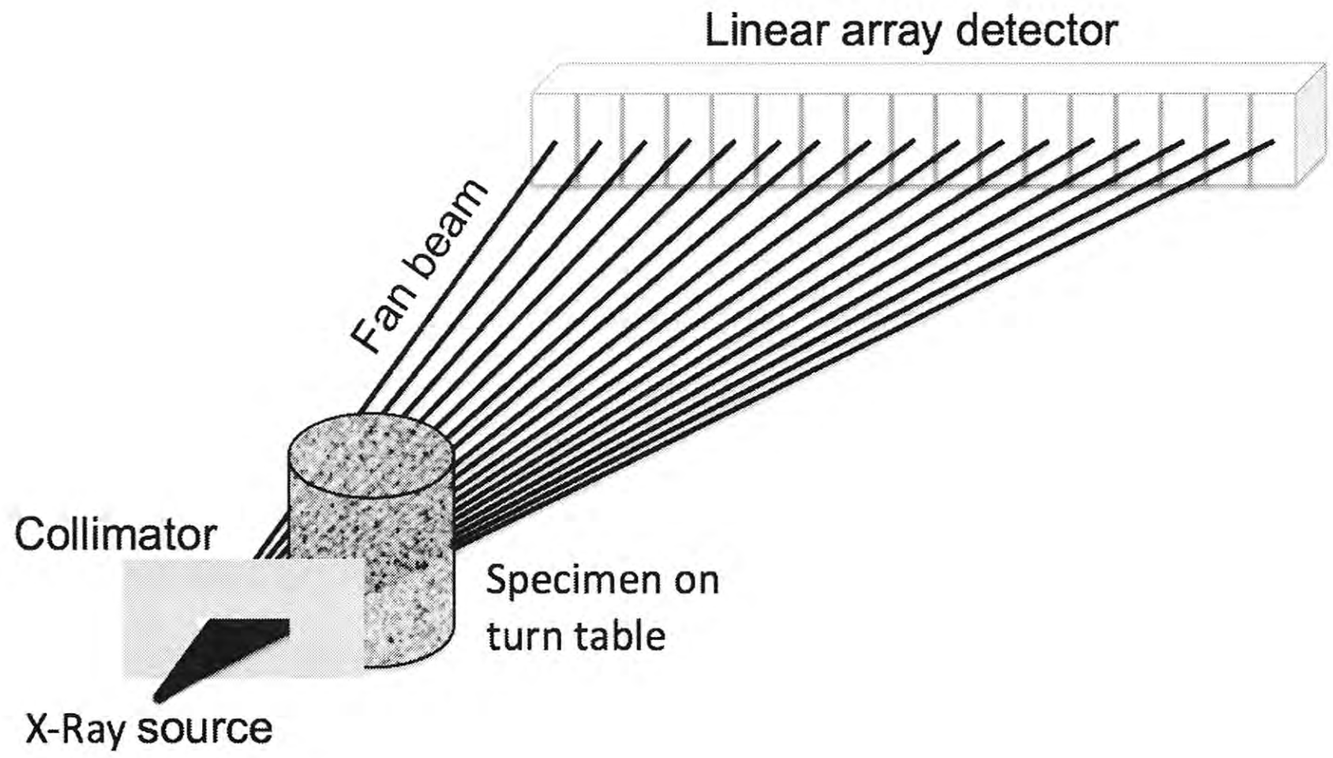

Figure 3.5. Schematic of X-Ray CT Imaging.
(Adapted from Ketcham, 2005a)

Each CT image is termed a 'slice', as it corresponds to what one would see if the

object were sliced along the scan plane. By gathering a stack of contiguous slices, data for a complete 3D volume can be obtained. Each slice represents a finite thickness of material, corresponding to the thickness of the collimated X-ray beam and detector array. Consequently, the pixels in CT images represent volume elements and are referred to as voxels (Ketcham, 2005a).

For the full asphalt mixture, two specimens for each of the four types of mixtures were scanned using the HRXCT for a total of eight full mix specimens. For the FAM mixtures, 10 specimens for each of three types of mixture were scanned using the HRXCT for a total of 30 FAM specimens. For each mixture design the 10 specimens comprised two from the inner core of the SGC compacted specimen, two from the outer core of the SGC compacted specimen, two from the beam specimen cored along the direction of compaction, two from the beam specimen cored along the transverse direction, and two from the Marshall compacted specimen. For each of the full or FAM specimens, a volume of approximately 15 mm x 15 mm x 8 mm, enclosing the middle third of the specimen, was scanned to obtain a total of 562 images each with a resolution of 1024 x 1024 pixels. The problems of beam hardening and ring artifacts were removed during post-construction phase. Figure 3.6 shows the typical matrix with scans of the specimen.

All images acquired using the HRXCT must be processed before conducting any kind of analysis. Matlab was used to process the images by cropping the images, removing noise and running a thresholding algorithm to separate the three components in the composite, i.e. mastic, air void and aggregate. The steps used for the image analysis are briefly described here. The two dimensional slice images obtained after scanning were 1024x1024 pixels in size. The images were cropped to a size of 512x512 pixels to obtain the region of interest and remove any unwanted information from the edges. The pixel intensity values of the images obtained in this manner varied from 0 to 165. In order to examine the fine details and visually distinguish between the fine features it is important to fully utilize the entire range of intensity values, i.e. 0 to 255. Therefore a contrast enhancement operation was performed on the cropped images.

All digital images, including the ones used in this study, contain some amount of noise. Eliminating noise while preserving the details of interest in the image is one of the challenges in image processing. Several different types of linear and nonlinear filtering tools are available to remove different types of noise that is typically present in digital images. Regardless of the type of filter, the output image should minimize noise without destroying the information of interest in the image. Based on a review documented in our earlier work

	FULL MIX	FAM MIX		
	COMPACTION METHOD	***SGC***	***BEAM***	***MARSHALL***
	SGC			
MIX 1	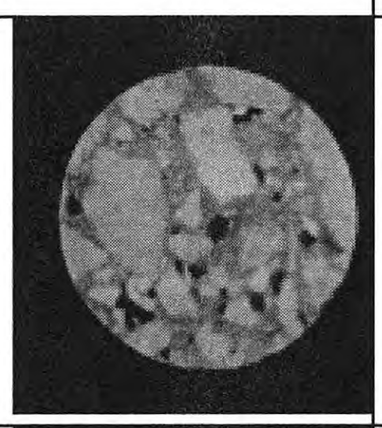	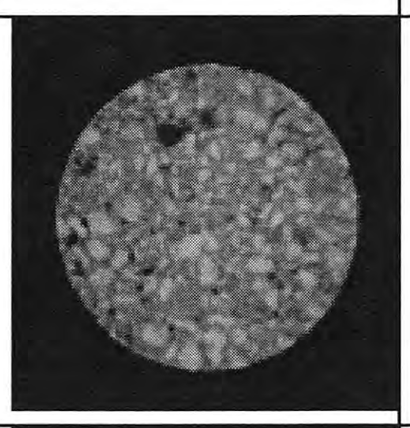	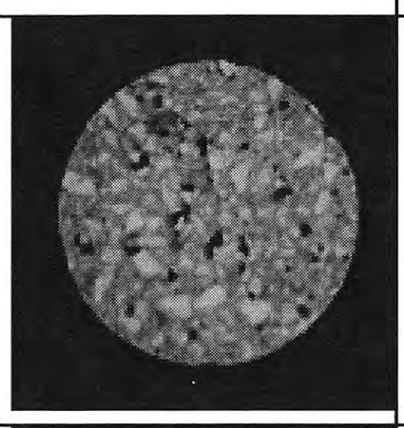	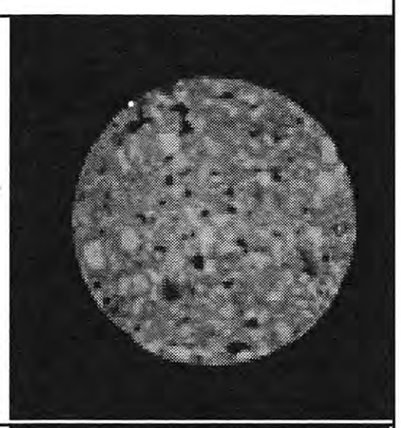
MIX 2	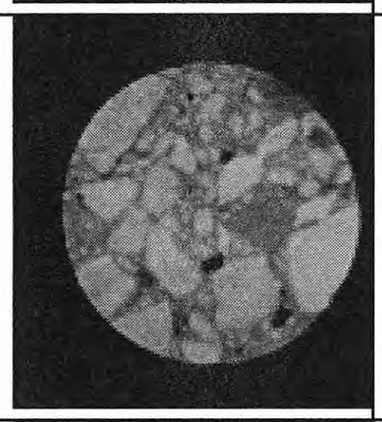	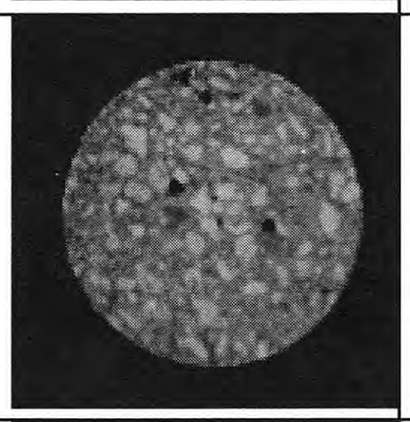	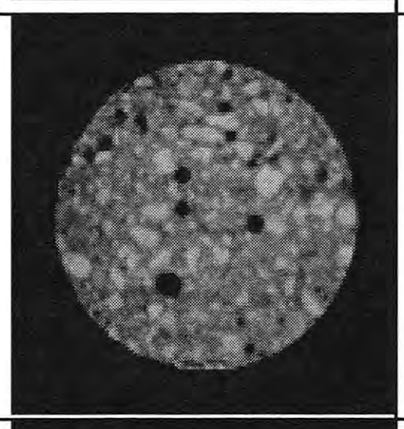	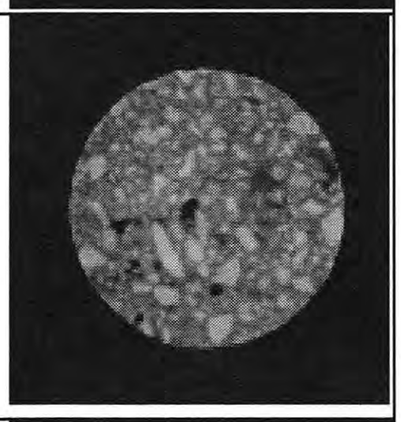
MIX 3	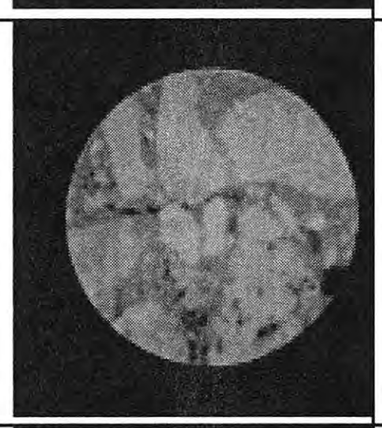	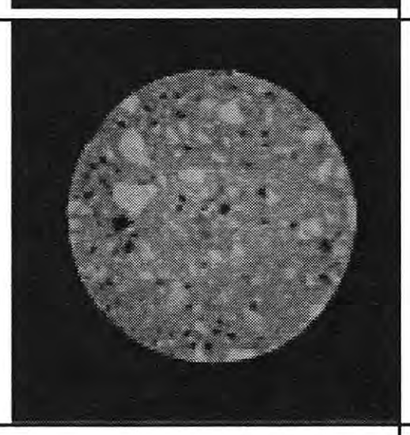	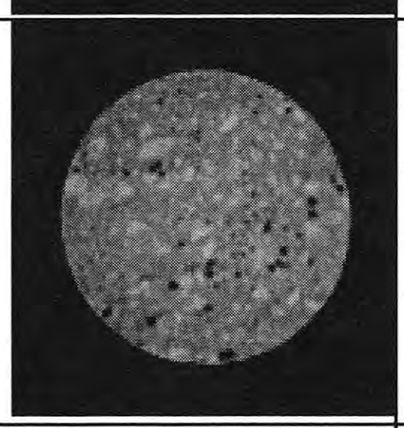	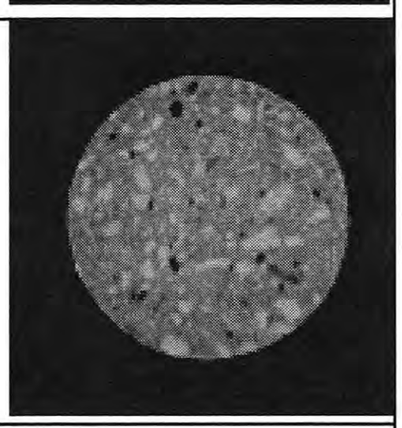
MIX 4	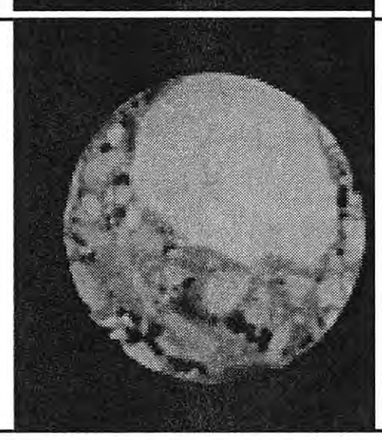			

Figure 3.6. Typical Slice Scans and Test Matrix.

(Bhasin et al., 2009) the median filtering technique was identified as the most optimal tool to remove noise. In the median filtering technique, the gray level of each pixel is replaced by the median of the gray level of all pixel values in the pixel's neighborhood (Russ, 2007). The neighborhood area, which is also referred to as the kernel, used in this study, was 3 by 3.

A typical mixture composite can be broken down into three components – aggregates, mastic (binder with fines or aggregates finer than 75 microns), and air. After noise reduction the next step was to convert the grayscale image to an image that contained only three pixel intensity values representing the three components within the composite. A thresholding operation was performed such that the end product had air represented by black pixels (pixel value 0), mastic represented by gray (pixel value 150) and aggregate represented by white (pixel value 255). The objective of the thresholding operation was to identify two pixel intensity values in the gray scale image that differentiate between these three components. The volumetric properties (volume of air void and volume of mastic) of each specimen were determined. An iterative process was used to determine the two pixel intensity values that differentiated between air voids, mastic, and the aggregates for a stack of 520 images that represent a volume of the specimen. The iterations were designed to minimize the difference between the volume percent of air voids and mastic computed using the stack of images to the values obtained experimentally. This procedure was based on the work of Zelelew et al. (2008).

One of the objectives of this study was to compare the microstructure of the mortar within a full asphalt mixture specimen to the microstructure of a corresponding FAM specimen. Based on a literature review, and as described in section 2.3 the metrics of choice selected to characterize the internal microstructure were based on the fabric tensor obtained using the star length distribution (SLD). The Quant3D program originally developed by Ketcham and co-workers was used to analyze images and characterize the microstructure of the mastic (2005a). The Quant3D program uses the processed images as an input and computes the SLD, fabric tensor, eigen values and eigen vectors for the component of interest. The SLD provides the average length of the component of interest (for specified number of points) along different orientations using a three dimensional rose diagram. For each specimen the 512 processed slice images were uploaded. The critical inputs for this program were as follows. The threshold range of values is used to describe the component of interest. For example, in the processed images, the air voids, mastic, and aggregates are represented using pixel intensity values of 0, 150, and 255, respectively. Therefore to analyze the microstructure of the mastic, a range of 145-155 was used to describe the material of interest in the composite. The number of directions was used to define the number of orientations along which the lengths were measured. For this study, 513 orientations that represent a uniform distribution on a sphere were selected. A total of 1000 points were randomly selected to make these measurements. Choosing the appropriate number of points

is an important parameter to obtain meaningful results. Selection of too many points results in very long computing time. In contrast, selection of too few points will not provide meaningful distributions.

Figure 3.7 illustrates a typical three dimensional rose diagram for the SLD. The average SLD is used to compute the fabric tensor using equation 2.3. The eigen vector and eigen values for this fabric tensor were also computed. Recall that the eigenvectors with the largest and smallest eigen values represent the direction vectors along which the moment of inertia is maximized and minimized representing the preferred direction of the matrix. In addition, the ratio of the maximum to the minimum eigen values is a measure of the degree of anisotropy.

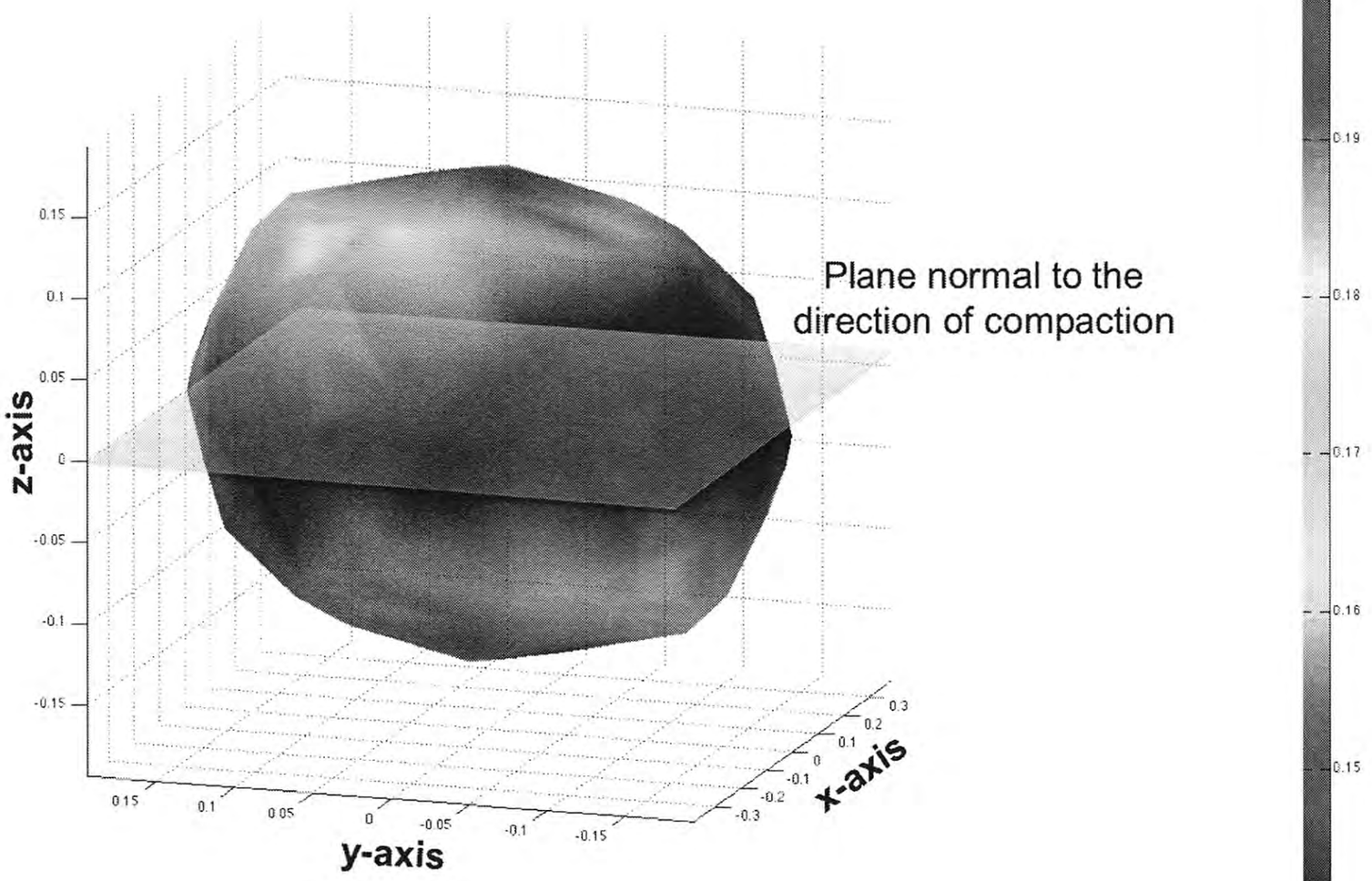

Figure 3.7. Typical Rose Diagram for the SLD with Respect to Axis of Compaction.

The results were used to obtain the four parameters that describe the internal microstructure or dimensional distribution of the mastic with the full asphalt mixture as well as the FAM specimens. As described in section 2.3 four metrics were derived from this analysis: degree of anisotropy, average star length, average coefficient of variation and orientation of the principal direction. Figures 3.8 and 3.9 illustrate the average SLD for the FAM specimens and the full asphalt mixtures, respectively. The absolute values for the

orientation of the principal direction varied mostly from 2 to 7 degrees and the results were statistically similar for all specimens and are not included here.

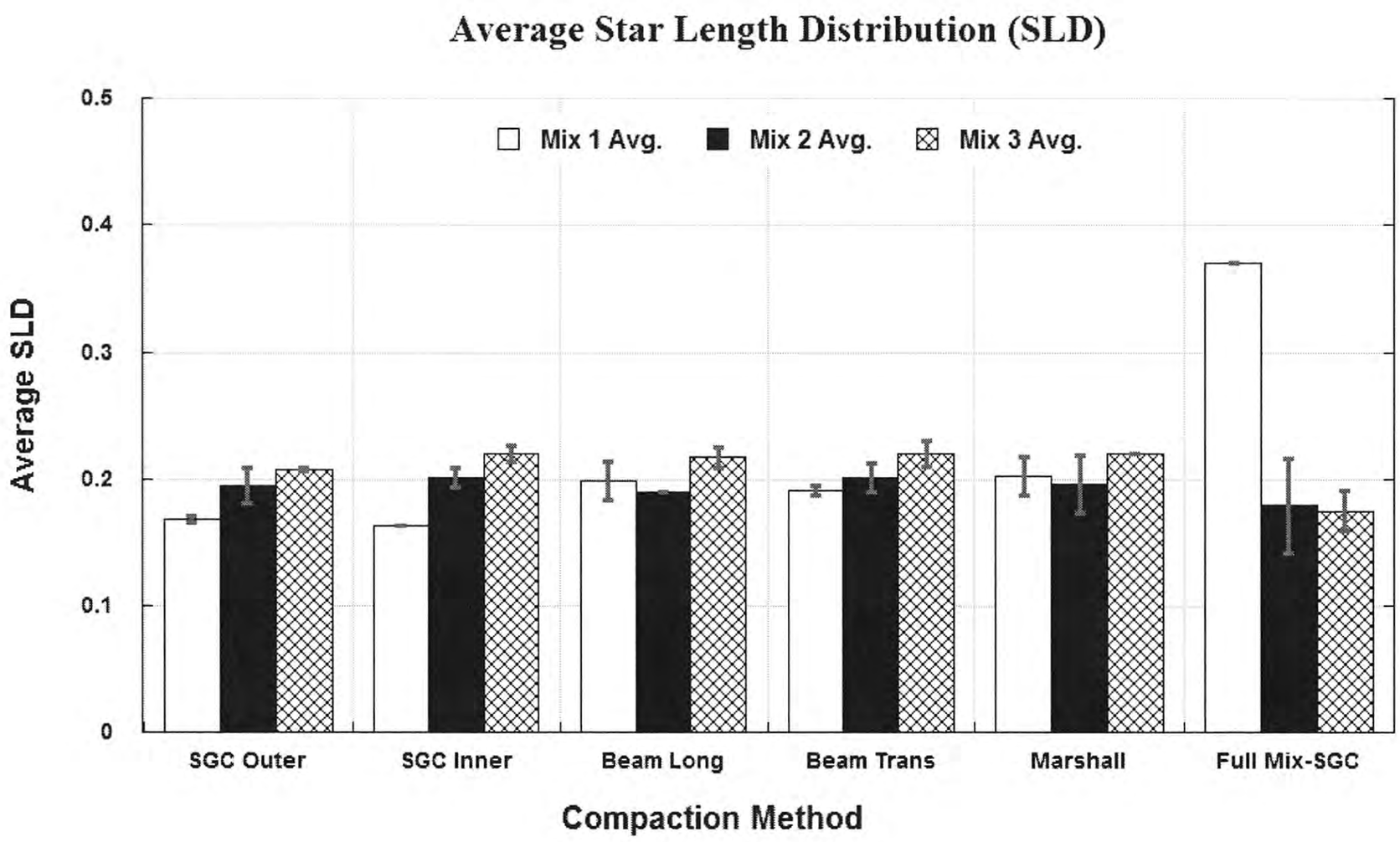

Figure 3.8. Average SLD Along Principal Direction for the FAM and Full Asphalt Mixtures.

Due to the limited scope of this project, only two specimens of each type were used for the X-ray tomography. Based on the results from this analysis, there appears to be some difference in the average SLD values depending on the mix type and method of compaction. However, in most cases these differences were not be significant statistically based on a t-test.

3.3 CHARACTERIZING ENGINEERING PROPERTIES

The FAM specimens were further subjected to DMA testing to evaluate the influence of mixture variable such as binder content and change in fine aggregate gradation as well the influence of the method of compaction. The DMA test was conducted by fixing one end of the FAM specimen and applying a torsional shear at the other end. Figure 3.10 illustrates the typical set up used for DMA testing.

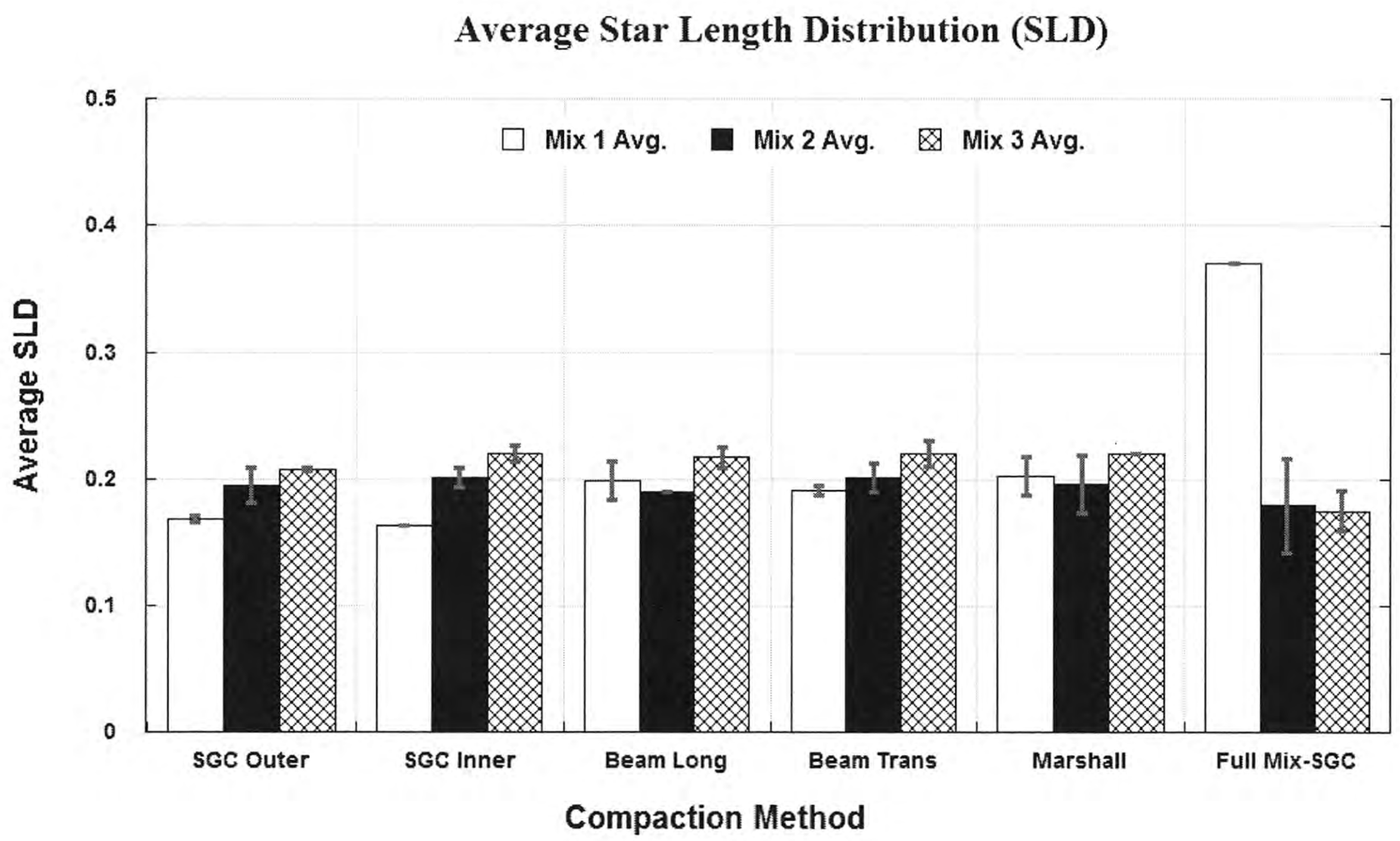

Figure 3.9. Average Degree of Anisotropy for the FAM and Full Asphalt Mixtures.

3.3.1 Undamaged properties

The linear viscoelastic or undamaged properties of the FAM specimens were measured by applying a sinusoidal load with a constant low stress amplitude and by measuring the dynamic shear modulus G^* and phase angle δ. The shear stress amplitude used was 10kPa and the frequency of loading was 5Hz. Figures 3.11 and 3.12 illustrate these two properties for the FAM specimens.

Both fine aggregate gradation and binder content had a significant influence on the mechanical properties of FAM. As expected, an increase in the asphalt binder content decreased the dynamic shear modulus and increased the phase angle of the FAM specimens. The influence of fine aggregate gradation on the dynamic shear modulus was not as significant as the asphalt binder content. Depending on the method of compaction the dynamic shear modulus and the phase angle either increased or decreased. The method of compaction had a significant influence on the dynamic shear modulus of the FAM specimens. For instance, the specimens prepared using Marshal compaction method had the highest modulus (G*).

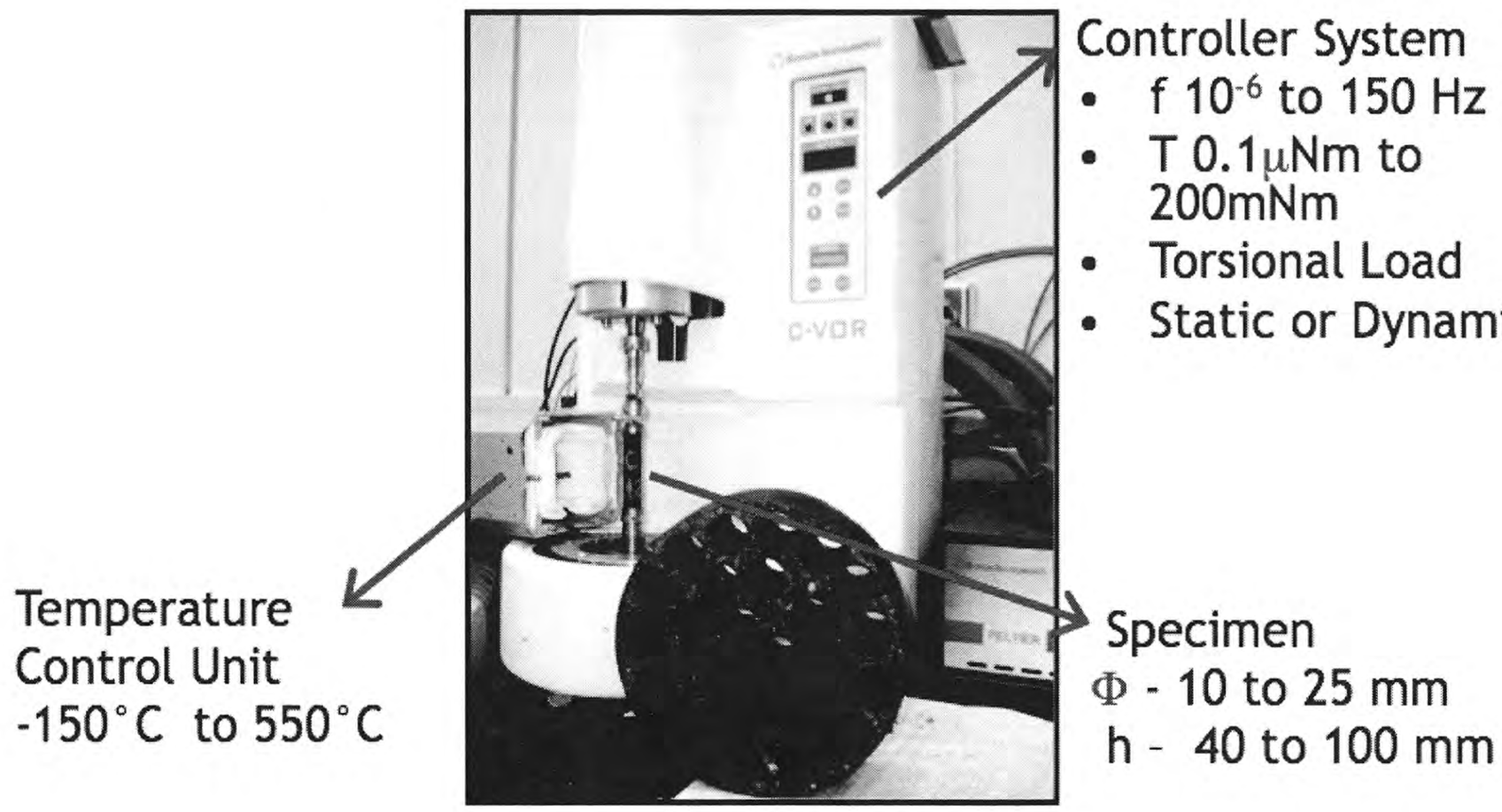

Figure 3.10. Setup of the DMA with a Typical Test Specimen.

The influence of three factors (binder content, fine aggregate gradation, and method of compaction) on the homogeneity and anisotropy of the specimen from a given method of compaction (SGC or beam) was evaluated. Comparing the two groups of specimens (inner and outer) fabricated using Superpave Gyratory Compactor, it was observed that with a minor exception there was no significant difference in the dynamic modulus or phase angle of the specimens from the inner core compared to the specimens from the outer core. Similarly, comparing two different groups of specimens prepared using the beam compactor (Longitudinal and Transversal), the FAM specimens were mostly isotropic at these stress levels in terms of the dynamic modulus and phase angle. At higher stress levels the FAM specimens from the beam compaction demonstrated slight anisotropy. However, the degree of anisotropy was not statistically significant. Figure 3.13 illustrates the dynamic shear modulus of the FAM specimens measured using a higher stress amplitude of 210 Kpa.

3.3.2 Fatigue crack growth

A time sweep test was conducted on the FAM specimens to characterize the fatigue cracking resistance. The time sweep was conducted by applying a sinusoidal wave form at 5Hz

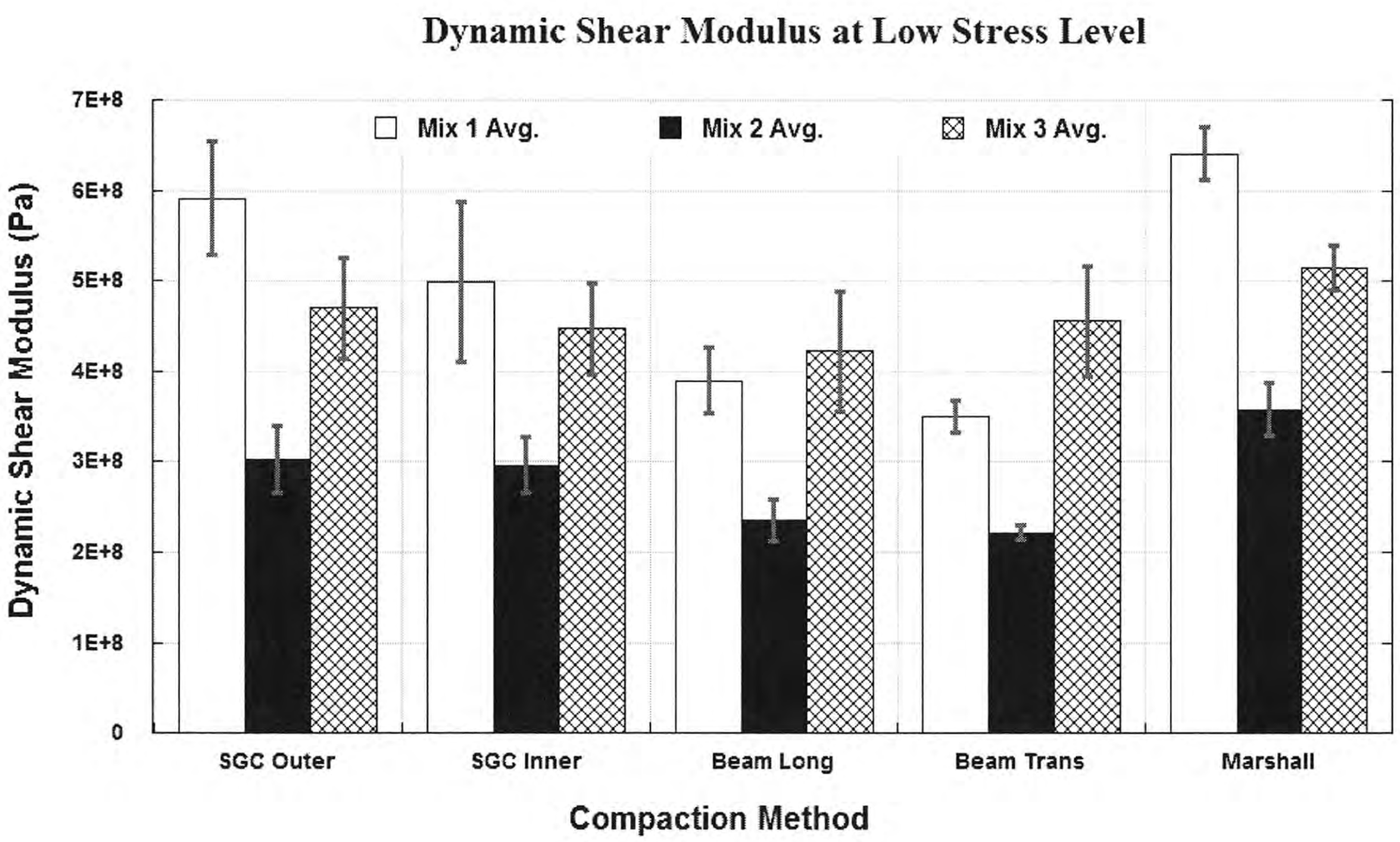

Figure 3.11. Average Linear Viscoelastic Complex Modulus for FAM Mixtures.

with a constant shear stress amplitude of 210kPa. The complex modulus of the specimen was recorded as a function of the number of load cycles. Due to the inherent variability associated with the fatigue test, the slope of the complex modulus, G^* versus $log\,(time)$ was used as a characteristic for the fatigue cracking resistance of the specimen. This parameter demonstrates the lowest amount of variability between replicates in a fatigue test. Figure 3.14 illustrates the typical reduction in G^* with time and power law fit with the relevant slope parameters. Figure 3.15 compares the rate of fatigue crack growth for the different FAM specimens.

The results indicate that the Marshal specimens experienced the highest rate of damage growth. As expected, an increase in the binder content decreased the rate of fatigue damage. The trend in terms of the rate of damage growth for different mix types and methods of compaction was very similar to the trends observed for the complex shear modulus at the high stress level. The effect of fine aggregate gradation was not as significant as asphalt binder content. Other than the FAM specimens cored in the transverse direction from the beam compacted specimen, Mix 1 and Mix 3 demonstrated similar fatigue cracking response. Recall that Mix 1 and Mix 3 represent the control and the fine adjusted mix,

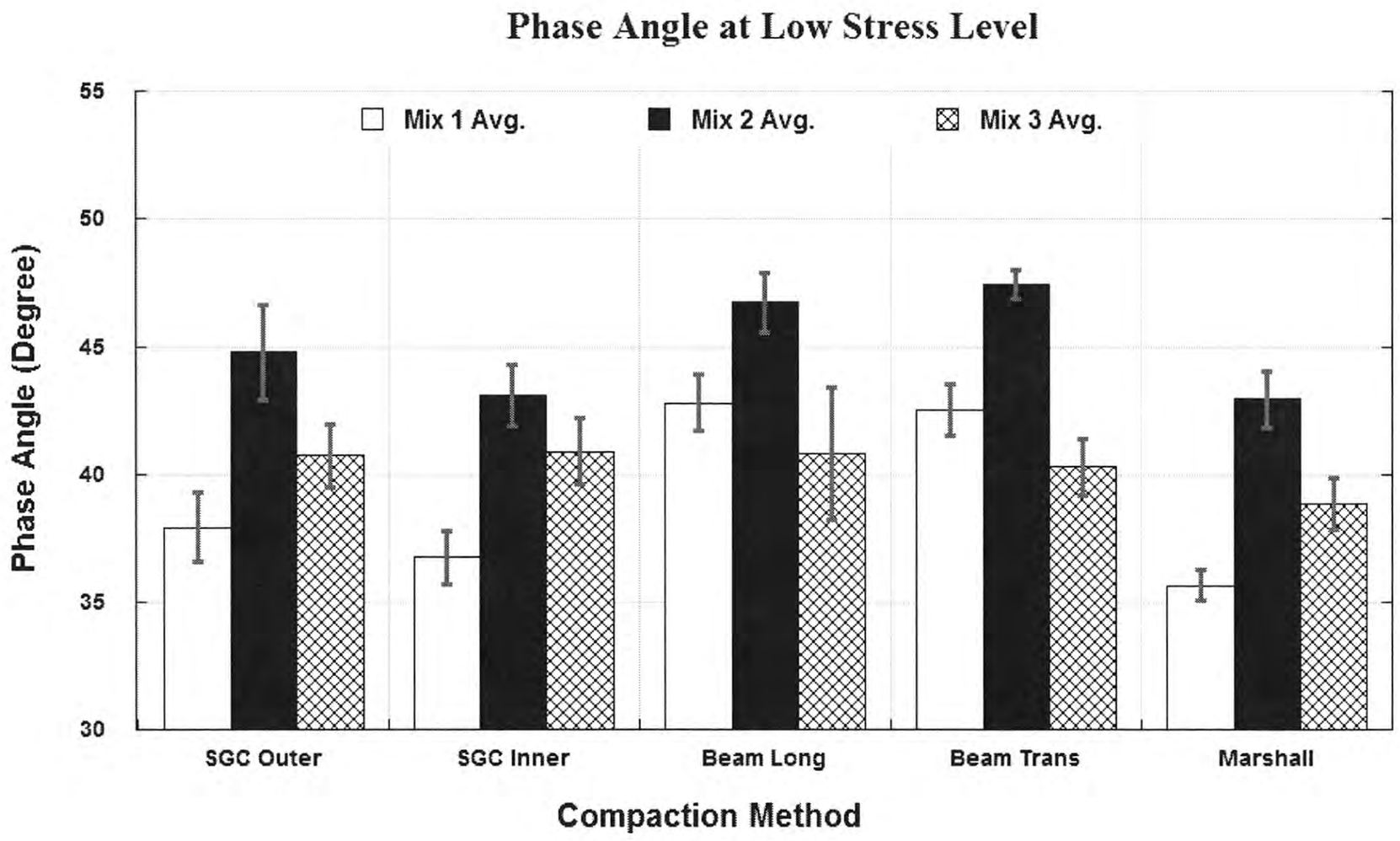

Figure 3.12. Average Linear Viscoelastic Phase Angle for FAM Mixtures.

respectively. The most significant difference between the fine adjusted and the control mix is the percentage of fines passing #200 sieve. Therefore, these results suggest that increasing the percentage of finer aggregates in the mix did not significantly influence the rate of fatigue crack growth. However, since this study included only a limited number of mixtures this finding must be further investigated in future work.

3.3.3 Healing characteristics

The self-healing characteristics of the FAM specimens were quantified based on the following method and metrics. A time sweep test following a sinusoidal wave form in shear was conducted with a frequency of 5Hz and constant stress amplitude of 210kPa. The test was continued until the measured complex shear modulus was 50% of the linear viscoelastic complex shear modulus measured at low stress amplitudes. At this stage, the test was stopped for a duration of 30 minutes. During this rest period, the linear viscoelastic complex shear modulus was measured by applying a shear stress following a sinusoidal wave form at a frequency of 5Hz and a stress amplitude of 10kPa for 50 cycles. This linear viscoelastic shear modulus was measured at 0.5, 1, 3, 5, 10 and 30 minutes after the start of

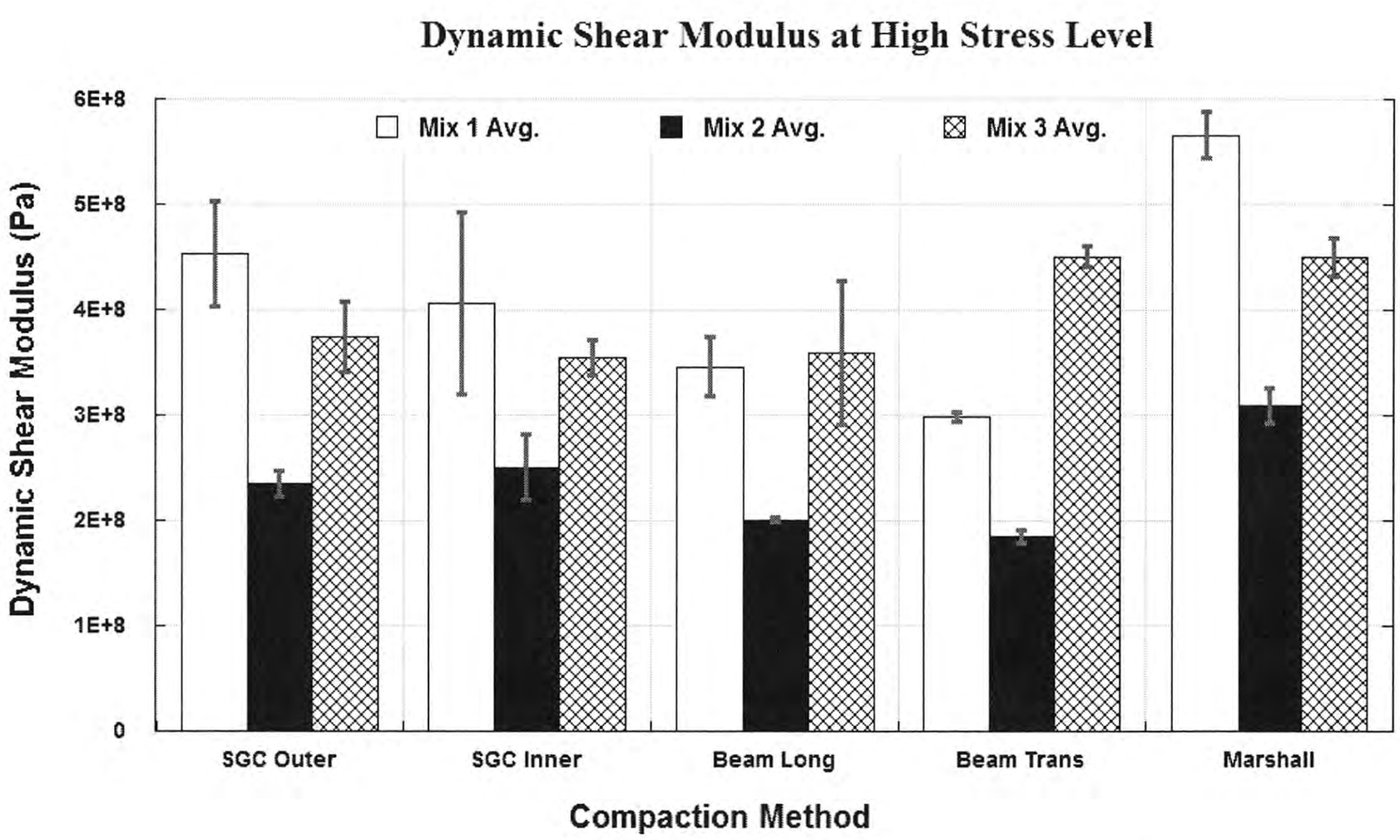

Figure 3.13. Average Viscoelastic Complex Modulus for FAM Mixtures at High Stress Levels.

the rest period. The increase in the linear viscoelastic shear modulus with time during the rest period was used as an indicator of the level of healing within the sample. The working assumption for this measurement was that the few load cycles applied from time to time during the rest period to measure the linear viscoelastic shear modulus will have a minimal affect on the healing process within the specimen. After the completion of the 30 minute rest period, the complex shear modulus of the specimen had significantly increased. At this time, the application of the high amplitude shear stress following a sinusoidal wave form with a frequency of 5Hz and stress amplitude of 210kPa was resumed. The high stress amplitude fatigue test was continued until the specimen again reached 50% of its linear viscoelastic shear stress amplitude. A second rest period of 30 minutes was introduced and the healing was recorded in terms of the linear viscoelastic complex shear modulus as before. The process was repeated for a total of four rest periods with the only exception that the fourth rest period was for 60 minutes instead of 30 minutes. After the fourth rest period the specimen was subjected to cyclic loading until failure.

The metric to quantify the healing characteristics of the FAM specimen was determined as follows. The healing or increase in the linear viscoelastic G^* during the rest period was

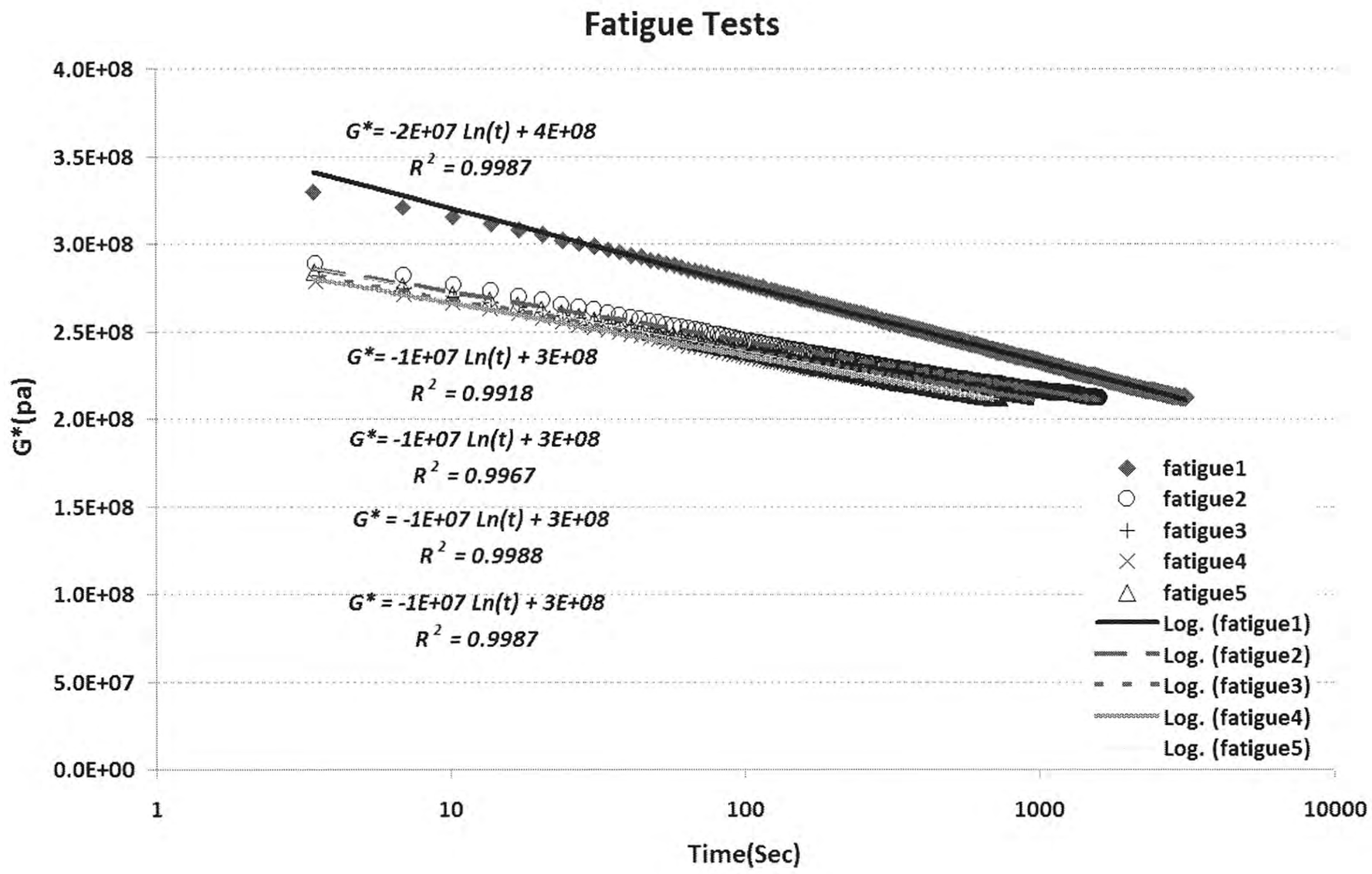

Figure 3.14. Typical Results from Fatigue Test using DMA.

plotted as a function of time during the rest period. This relationship was found to fit the following model:

$$\log(G^*) = c\log(t) + d \tag{3.1}$$

where, c and d are material constants and t is time. A total of four relationships and four sets of parameters could be plotted corresponding to each one of the four rest periods. Examination of some results showed that the material parameters c and d did not change significantly from the first rest period to the fourth. Therefore, for the remainder of the work presented in this report, the parameter d from the first rest period is used as the metric that characterizes the healing properties of that specimen. Figures 3.16 and 3.17 illustrates the healing curves from the four rest periods along with the parameters indicated in equation 3.1. Figure 3.18 compares the healing characteristics for the different FAM specimens.

Results demonstrate that an increase in the asphalt content or fines do not necessarily improve the healing characteristics of the FAM specimen. This can be explained as follows. The average dimensions of the mastic between the fine aggregate particles or average SLD has a significant influence on the fracture and healing properties of the asphalt mixture. In

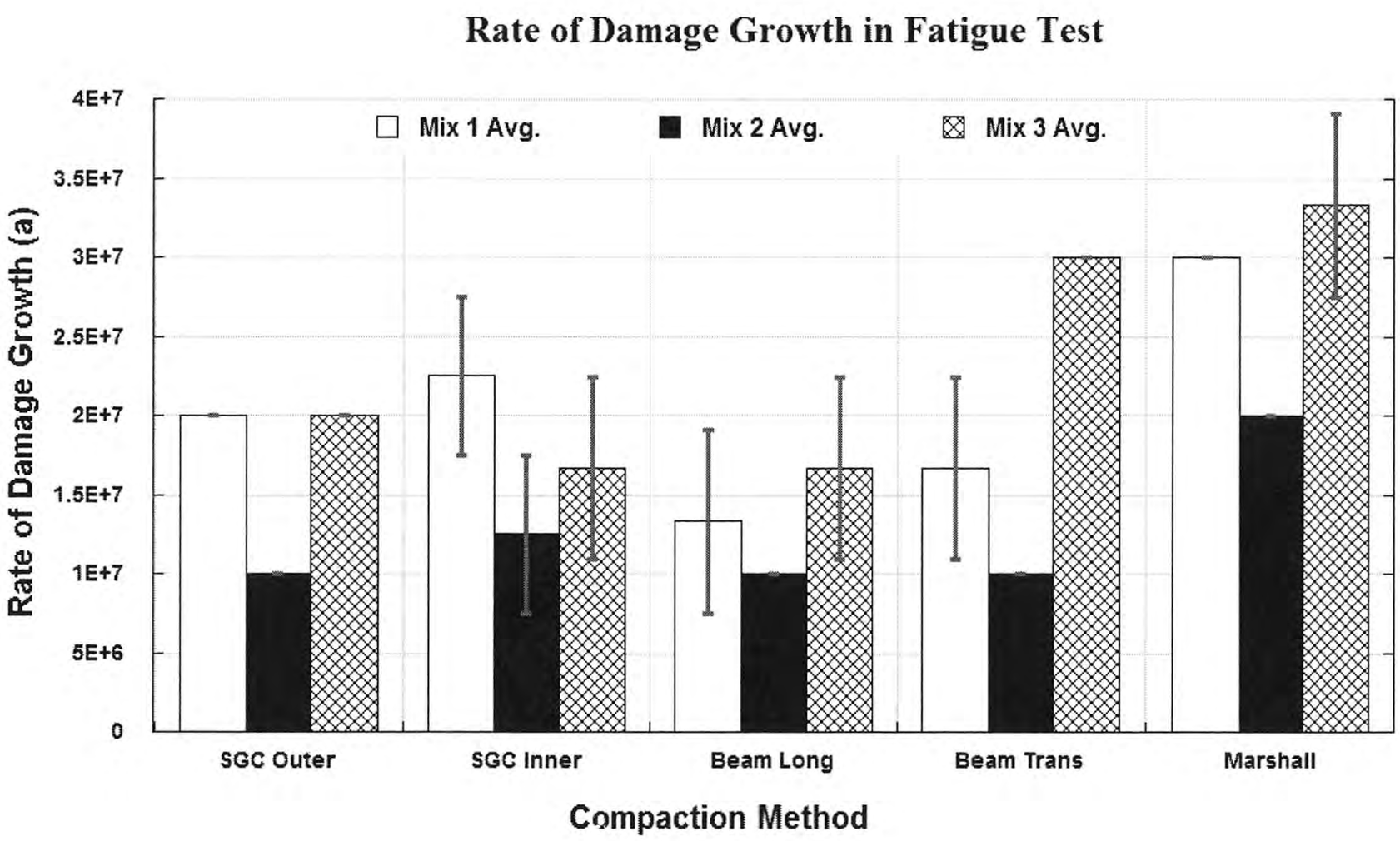

Figure 3.15. Average Fatigue Crack Growth Rate for FAM Mixtures.

a previous work by these authors, an increase in the binder content in asphalt mixtures did not necessarily increase the average binder volume between the fine aggregate particles. As shown in the results described in section 2.1, the average SLD for the full mixture with high mastic volume was in fact less than the average SLD for the control mixture. Similarly, the average SLD for the FAM specimens with high mastic volume (Mix 2 and Mix 3) was not significantly different compared to the control mix, based on the number of replicates. A more uniformly dispersed mastic with smaller average dimensions can demonstrate improved fatigue cracking resistance on account of and increased tensile strength of the binder due to higher confining pressures. Similarly, self-healing in the asphalt is strongly influenced by the crack size and volume of asphalt around the crack tip. Smaller cracks will demonstrate a higher rate of self-healing. At the same time, smaller volume of asphalt surrounding the crack (smaller average SLD dimensions) will result in reduced rate of self-healing because of an increased local stiffness surrounding the crack-tip. These mechanisms, combined with the results that demonstrate that the average dimensions of the mastic distributed between the aggregate particles do not vary significantly between the three mixtures, are consistent with the observation that the healing characteristics of Mixes

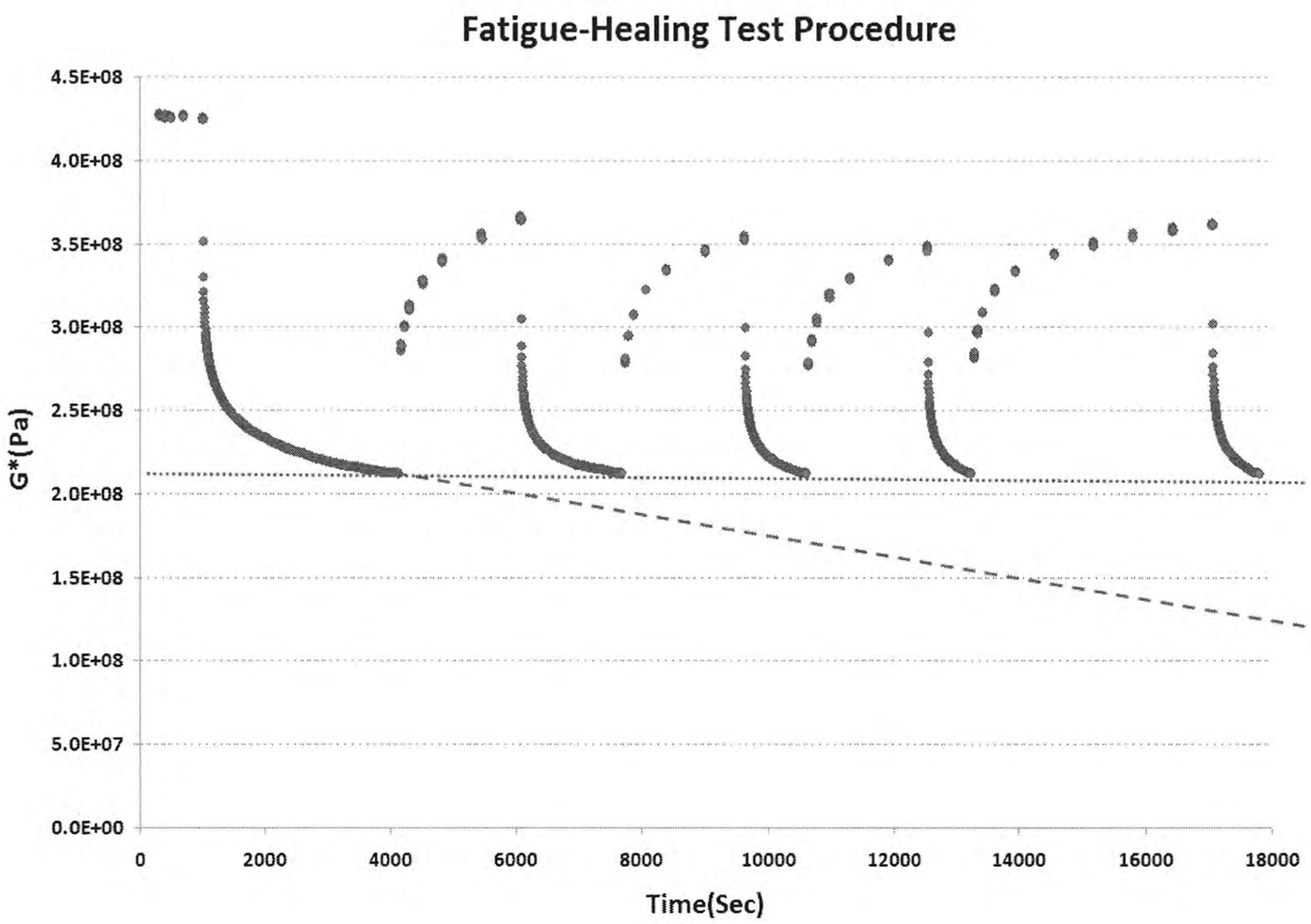

Figure 3.16. Typical Fatigue Test with Rest Periods.

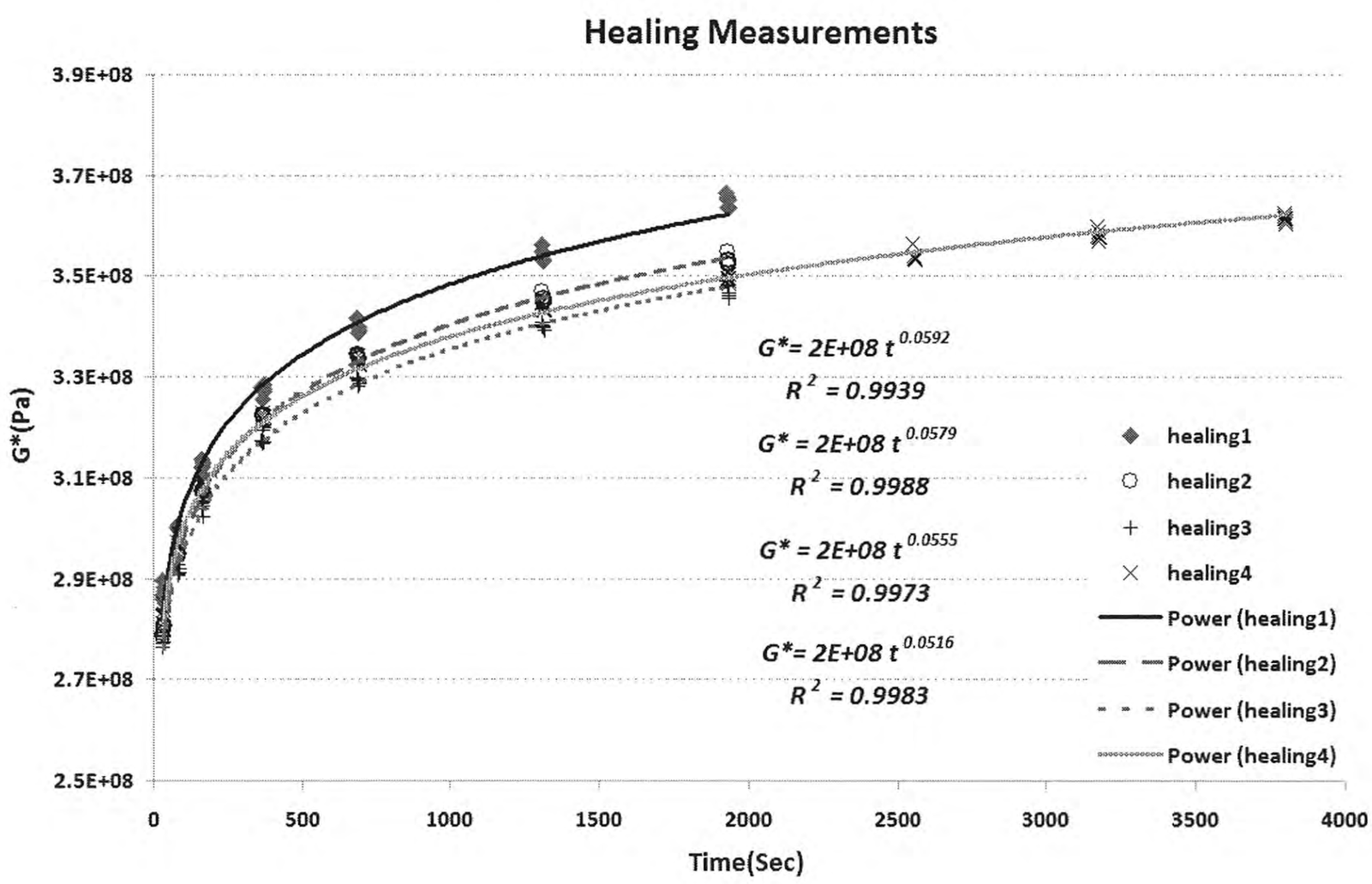

Figure 3.17. Typical Healing vs. Time Curves From Four Rest Periods.

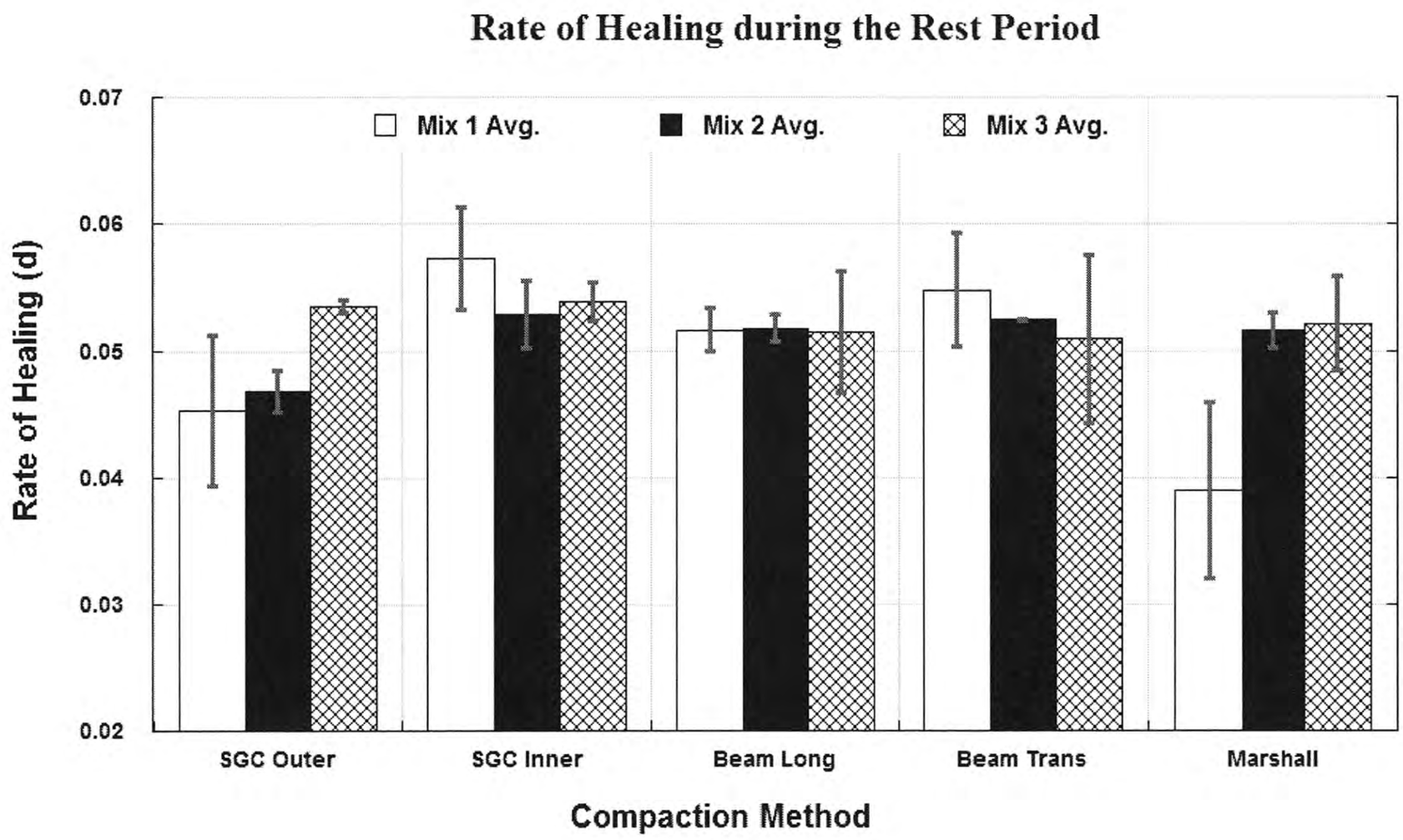

Figure 3.18. Average Healing Characteristic Parameter for FAM Mixtures.

2 and 3 were similar to the healing characteristic of Mix 1, despite the higher percentage of the asphalt binder.

CHAPTER 4. CONCLUSIONS

The objectives of this study were to compare the internal microstructure of the mortar from a full asphalt mixture to the internal microstructure of a FAM specimen with a corresponding volumetric mix design. Another objective of this study was to evaluate the influence of mixture properties and methods of compaction on the engineering properties of the FAM specimens. The results from this study, although limited in number, indicate that in most cases the SGC compacted FAM specimen had a microstructure that most closely resembled the microstructure of the mortar within a full asphalt mixture. Results also demonstrate that a change in the fine aggregate fraction of the aggregate did not significantly change the fatigue cracking resistance of the FAM specimens. The fatigue cracking characteristics of the FAM specimens were strongly influenced by the binder content; the percentage of fines did not have a significant influence.

The key finding from this study was that the healing characteristic of the three different types of FAM mixes was not significantly different. This is despite the fact that the percentage of fines in one of the mixes and the percentage of binder in the other mix was higher than those in the control mix. This indicates that the healing rate is mostly dictated by the type of binder and not significantly influenced by the gradation or binder content, as long as the volumetric distribution of the mastic was the same. In other words, the limited results from this study indicate that the inherent healing characteristics of the asphalt binder plays a more significant role relative to other properties (e.g. volumetrics) in the overall fatigue cracking resistance of the asphalt mixture.

REFERENCES

Bhasin, A., Badgekar, S., and Izadi, A. 2009. Quantitative characterization of asphalt mixtures. Final Report 476660-00070-1, Southwest Region University Transportation Center.

Bhasin, A., Little, D. N., Bommavaram, R., and Vasconcelos, K. L. 2008. A framework to quantify the effect of healing in bituminous materials using material properties. *International Journal of Road Materials and Pavement Design*, EATA 08:219–242.

Branco, V. C., Masad, E., Bhasin, A., and Little, D. N. 2008. Fatigue analysis of asphalt mixtures independent of mode of loading. *Transportation Research Record*, 2057:149–156.

Brinson, H. F. and Brinson, L. C. 2008. *Polymer Engineering Science and Viscoelasticity*. Springer.

Caro, S., Masad, E., Airey, G. D., Bhasin, A., and Little, D. N. 2008. Probabilistic analysis of fracture in asphalt mixtures caused by moisture damage. *Transportation Research Record*, In Press.

Carpenter, S. H. and Shen, S. 2006. A dissipated energy approach to study HMA healing in fatigue. In *85th Annual Meeting of the Transportation Research Board*, Washington D.C.

Cherepanov, G. P. 1968. Cracks in solids. *International Journal of Solids and Structures*, 4(8):811 – 831.

Ferry, J. D. 1980. *Viscoelastic Properties of Polymers*. Wiley.

Huang, C., Masad, E., Muliana, A., and Bahia, H. 2007. Nonlinearly viscoelastic analysis of asphalt mixes subjected to shear loading. *Mechanics of Time-Dependent Materials*, 11(2):91–110.

Ketcham, R. A. 2005a. Computational methods for quantitative analysis of three-dimensional features in geological specimens. *Geosphere*, 1(1):32–41.

Ketcham, R. A. 2005b. Three-dimensional grain fabric measurements using High-Resolution X-Ray computed tomography. *Journal of Structural Geology*, 27:1217–1228.

Ketcham, R. A. and Carlson, W. D. 2001. Acquisition, optimization and interpretation of x-ray computed tomographic imagery: Applications to the geosciences. *Computers & Geosciences*, 27(4):381–400.

Kim, B. and Roque, R. 2006. Evaluation of healing property of asphalt mixture. In *85th Annual Meeting of the Transportation Research Board*, Washington, D.C.

Kim, Y. and Little, D. N. 2005. Development of specification type tests to assess the impact of fine aggregate and mineral filler on fatigue damage. Technical Report 0-1707-10, Texas Transportaion Institute.

Kim, Y. R., Little, D. N., and Lytton, R. L. 2004. Effect of moisture damage on material properties and fatigue resistance of asphalt mixtures. *Transportation Research Record: Journal of the Transportation Research Board*, 1891:48–54.

Kim, Y. R., Little, D. N., and Song, I. 2003. Effect of mineral FIllers on fatigue resistance and fundamental material characteristics: Mechanistic evaluation. *Transportation Research Record: Journal of the Transportation Research Board*, 1832:1–8.

Lakes, R. 2009. *Viscoelastic Materials*. Cambridge University Press.

Little, D. N., Lytton, R. L., Williams, A. D., and Chen, C. W. 2001. Microdamage healing in asphalt and asphalt concrete, volume i: Microdamage and microdamage healing, project summary report. Technical Report FHWA-RD-98-141, Texas Transportation Institution, College Station, TX.

Maillard, S., de La Roche, C., Hammoum, F., Gaillet, L., and Such, C. 2004. Experimental investigation of fracture and healing at Pseudo-Contact of two aggregates. In *3rd Euroasphalt and Eurobitume Congress*, Vienna.

Masad, E., Branco, V. C., and Little, D. N. 2006. Fatigue damage: Analysis of mastic fatigue damage using stress controlled and strain controlled test. Technical Report 473630, Texas Transportation Institute in cooperation with Federal Highway Administration and Western Research Institute.

Masad, E. and Button, J. 2004. Implications of experimental measurements and analyses of the internal structure of Hot-Mix asphalt. *Transportation Research Record: Journal of the Transportation Research Board*, 1891:212–220.

Masad, E., Huang, C., Airey, G., and Muliana, A. 2008. Nonlinear viscoelastic analysis of unaged and aged asphalt binders. *Construction and Building Materials*, 22(11):2170–2179.

Masad, E., Muhunthan, B., Shashidhar, N., and Harman, T. 1999. Internal structure characterization of asphalt concrete using image analysis. *Journal of Computing in Civil Engineering*, 13(2):88–95.

Odgaard, A. 1997. Three-dimensional methods for quantification of cancellous bone architecture. *Bone*, 20(4):315 – 328.

Rice, J. R. 1968. A path independent integral and the approximate analysis of strain concentration by notches and cracks. *Journal of Applied Mechanics*, 35:379–386.

Russ, J. 2007. *The image processing handbook*. CRC/Taylor and Francis, Boca Raton, 5th ed. edition.

Schapery, R. A. 1975a. A theory of crack initiation and growth in viscoelastic media, i. theoretical development. *International Journal of Fracture*, 11(1):141–159.

Schapery, R. A. 1975b. A theory of crack initiation and growth in viscoelastic media, II. approximate methods of analysis. *International Journal of Fracture*, 11(3):369–388.

Schapery, R. A. 1975c. A theory of crack initiation and growth in viscoelastic media, III. analysis of continuous growth. *International Journal of Fracture*, 11(4):549–562.

Schapery, R. A. 1984. Correspondence principles and a generalized j integral for large deformation and fracture analysis of viscoelastic media. *International Journal of Fracture*, (25):195–223.

Watson, G. S. 1966. The statistics of orientation data. *The Journal of Geology*, 74(5):786–797.

Wineman, A. S. and Rajagopal, K. R. 2000. *Mechanical Response of Polymers: An Introduction*. Cambridge University Press, Cambridge.

Zelelew, H., Papagiannakis, A. T., and Masad, E. 2008. Application of digital image processing techniques for asphalt concrete mixture images. In *The 12th International Conference of IACMAG*, pages 119–124, Goa, India.

Zollinger, C. 2005. *Application of Surface Energy Measurements to Evaluate Moisture Susceptibility of Asphalt and Aggregates*. PhD thesis, Texas A&M University.

APPENDIX A. FAM DESIGN AS A DERIVATIVE OF A FULL MIX

The following two considerations are defined prior to designing the FAM mixture:

1. The gradation of the FAM mixture basically follows the same gradation as the full asphalt mixture it is designed to represent with only the portion of aggregate that pass #16 sieve.

2. The binder content by weight percent of the aggregates passing #16 sieve in the FAM mixture is the same as the binder content by weight percent of the aggregates passing #16 sieve in the full asphalt mixture minus the binder absorbed by the coarse aggregate.

The following example illustrates the procedure that was used to design a typical FAM mixture as a derivative of a full asphalt mixture.

A HMA mixture that will serve as the basis was first selected. An example gradation is provided in Table A.1.

Table A.1. Gradation for the full asphalt mixture.

Aggregate type	Sieve Size	Percent in the mix	Weight (g)	Cumulative weight (g)
Delta-Rock	3/4" - 3/8"	25.4%	1,946.7	1,946.7
Centex-Rock	3/4" - 3/8"	4.3%	329.6	2,276.3
Centex-Rock	3/8" - #4	17.0%	1,302.9	3,579.2
Centex-Rock	#4 - #8	15.9%	1,218.6	4,797.8
Centex-Rock	#8 - #16	9.5%	728.1	5,525.9
Centex-Rock	#16 - #30	9.4%	720.4	6,246.3
Centex-Rock	#30 - #50	6.7%	513.5	6,759.8
Centex-Rock	#50 - #200	8.3%	636.1	7,395.9
Centex-Rock	Pass #200	3.5%	268.2	7,664.1
BINDER	PG 64-22	4.2%	336.0	

The following information was obtained:

- Total weight of aggregates W_s = 7664.1 g

- Aggregate gradation (% passing vs. sieve size): as shown in Table A.1

- Percentage of binder $P_b = 4.2\%$
- Maximum specific gravity of a mix, G_{mm-R16}, using only aggregates retained on #16 sieve and any known amount of binder that is sufficient to completely coat the aggregate particles, P_{b-R16}. In this example G_{mm} was measured to be 2.442 and P_{b-R16} was 4.8%.
- The bulk specific gravity, G_{sb-R16}, of aggregates retained on #16 sieve i.e. 2.54 for this example.
- The specific gravity of the binder, G_b, i.e. 1.03 for this example.
- The G_{se-R16} of aggregates retained on #16 was calculated using the following equation:

$$G_{se-R16} = \frac{100 - P_{b-R16}}{\frac{100}{G_{mm-R16}} - \frac{P_{b-R16}}{G_b}} \tag{A.1}$$

- The percent weight of binder absorbed into aggregates retained on #16 was calculated using the following equation:

$$P_{ba-R16} = \frac{(100 * G_b)(G_{se-R16} - G_{sb-R16})}{(G_{se} * G_{sb-R16})} \tag{A.2}$$

- Weight of the binder absorbed in the coarse aggregate fraction is computed as:

$$W_{ba-R16} = P_{ba-R16} * Weight\ of\ aggregates\ retained\ on\ \#16 \tag{A.3}$$

- Finally, weight of the binder in the FAM is determined as:

$$W_{b-FAM} = W_b - W_{b-R16} \tag{A.4}$$

- The Table below lists the final mix design for this FAM mix.

Table A.2. Mix design for the FAM.

Aggregate type	Sieve Size	Percent in the mix	Weight (g)	Cumulative weight (g)
Centex-Rock	#16 - #30	30.0%	720.4	720.4
Centex-Rock	#30 - #50	21.4%	513.5	1,233.9
Centex-Rock	#50 - #200	26.5%	636.1	1,870.0
Centex-Rock	Pass #200	11.2%	268.2	2,138.2
BINDER	PG 64-22	11.0%	265.3	2,403.5